Oxygenation of offshore Southern California marine basins through the Holocene

Hannah M Palmer[1,1], Tessa M Hill[1,1], Esther Kennedy[2,2], Peter D Roopnarine[3,3], Sonali Langlois[4,4], Katherine Reyes[5,5], and Lowell Stott[6,6]

[1]University of California, Davis
[2]University of California Davis
[3]California Academy of Sciences
[4]Santa Rosa Junior College
[5]Dominican University of California
[6]University of Southern California

November 30, 2022

Abstract

In the face of ongoing marine deoxygenation, understanding timescales and drivers of past oxygenation change is of critical importance. Marine sediment cores from tiered silled basins provide a natural laboratory to constrain timing and implications of oxygenation changes across multiple depths. Here, we reconstruct oxygenation and environmental change over time using benthic foraminiferal assemblages from sediment cores from three basins across the Southern California Borderlands: Tanner Basin (EW9504-09PC, 1194 m water depth), San Nicolas Basin (EW9504-08PC, 1442 m), and San Clemente Basin (EW9504-05PC ,1818 m). We utilize indicator taxa, community ecology, and an oxygenation transfer function to reconstruct past oxygenation, and we directly compare reconstructed dissolved oxygen to modern measured dissolved oxygen. We generate new, higher resolution carbon and oxygen isotope records from planktic (Globigerina bulloides) and benthic foraminifera (Cibicides mckannai) from Tanner Basin. Geochemical and assemblage data indicate limited ecological and environmental change through time in each basin across the intervals studied. Early to mid-Holocene (11.0-4.7 ka) oxygenation below 1400 m (San Clemente and San Nicolas) was relatively stable and reduced relative to modern. San Nicolas Basin experienced a multi-centennial oxygenation episode from 4.7-4.3 ka and oxygenation increased in Tanner Basin gradually from 1.7-0.8 ka. Yet across all three depths and time intervals studied, dissolved oxygen is consistently within a range of intermediate hypoxia (0.5-1.5 ml L-1 [O2]). Variance in reconstructed dissolved oxygen was similar to decadal variance in modern dissolved oxygen and reduced relative to Holocene-scale changes in shallower basins.

Ecological and environmental stability in offshore Southern California Marine Basins through the Holocene

Hannah M. Palmer[1,2], Tessa M. Hill[1,2], Esther G. Kennedy[1,2], Peter D. Roopnarine[3], Sonali Langlois[4], Katherine R. Reyes[5], and Lowell D. Stott[6]

1. Earth and Planetary Sciences, University of California, Davis
2. Bodega Marine Laboratory, University of California, Davis
3. California Academy of Sciences
4. Santa Rosa Junior College
5. Dominican University of California
6. University of Southern California

Corresponding author: Hannah M. Palmer (hmpalmer@ucdavis.edu)

Key Points:

- In the Southern California Borderlands, oxygenation below 1400 m was stable and reduced relative to modern from 11.0-4.7 ka
- San Nicolas Basin experienced an oxygenation episode from 4.7-4.3 ka and oxygenation in Tanner Basin increased at 1.7 ka relative to 5.4-1.7 ka
- Variance in reconstructed Holocene dissolved oxygen concentration is similar to decadal scale variance in modern dissolved oxygen

Abstract

In the face of ongoing marine deoxygenation, understanding timescales and drivers of past oxygenation change is of critical importance. Marine sediment cores from tiered silled basins provide a natural laboratory to constrain timing and implications of oxygenation changes across multiple depths. Here, we reconstruct oxygenation and environmental change over time using benthic foraminiferal assemblages from sediment cores from three basins across the Southern California Borderlands: Tanner Basin (EW9504-09PC, 1194 m water depth), San Nicolas Basin (EW9504-08PC, 1442 m), and San Clemente Basin (EW9504-05PC ,1818 m). We utilize indicator taxa, community ecology, and an oxygenation transfer function to reconstruct past oxygenation, and we directly compare reconstructed dissolved oxygen to modern measured dissolved oxygen. We generate new, higher resolution carbon and oxygen isotope records from planktic (*Globigerina bulloides*) and benthic foraminifera (*Cibicides mckannai*) from Tanner Basin. Geochemical and assemblage data indicate limited ecological and environmental change through time in each basin across the intervals studied. Early to mid-Holocene (11.0-4.7 ka) oxygenation below 1400 m (San Clemente and San Nicolas) was relatively stable and reduced relative to modern. San Nicolas Basin experienced a multi-centennial oxygenation episode from 4.7-4.3 ka and oxygenation increased in Tanner Basin gradually from 1.7-0.8 ka. Yet across all three depths and time intervals studied, dissolved oxygen is consistently within a range of intermediate hypoxia (0.5-1.5 ml L^{-1} [O_2]). Variance in reconstructed dissolved oxygen was similar to decadal variance in modern dissolved oxygen and reduced relative to Holocene-scale changes in shallower basins.

Plain Language Summary

Globally, marine oxygenation is declining with detrimental impacts to ecosystems and economies. To better understand the drivers and consequences of ocean oxygen change, we can examine the fossil record to identify how oxygenation changed in the past. Specifically, we use the relative abundance and chemistry of microfossils (i.e., foraminifera) to reconstruct past oxygenation. Here, we examined microfossils from three sediment cores in three basins (Tanner, San Nicolas, San Clemente) off the coast of Southern California. Marine dissolved oxygen (below 1400 m water depth) was relatively stable and lower than modern from 11,000 to 4,700 years before present. San Nicolas Basin experienced a multi-centennial oxygenation episode from 4,700-4,300 years before present and oxygenation increased in Tanner Basin gradually from 2,000-800 years before present. When compared to modern, the range of values of reconstructed oxygen through the entire time studied (thousands of years) is similar to the range of values of modern oxygen at the same depths, indicating that the changes in the last ten thousand years were similar to the amount of change occurring on annual and decadal timescales in the modern ocean.

1 Introduction

1.1 Marine oxygenation in the past and present

At present, global marine oxygenation is declining due to anthropogenic climate change, with important implications for benthic and pelagic ecosystems (Breitburg et al., 2018; Oschlies et al., 2018; Schmidtko et al., 2017). Ocean oxygenation, particularly at depth, is an important driver of ecosystem zonation, and expansion of oxygen minimum zones (OMZ) is a current threat to global marine ecosystems (Breitburg et al., 2018; Helly & Levin, 2004; Stramma, Schmidtko, et al., 2010). Deoxygenation at depth can be driven by several processes: increased export of organic matter from surface to depth leading to increased respiration below the photic zone, increased stratification (often due to surface warming) reducing ventilation at depth, warming surface temperatures reducing rates of diffusion of atmospheric oxygen into surface waters, and changes in the source, current velocity, or oxygenation of intermediate waters (Levin et al., 2009; Oschlies et al., 2018; Stramma, Schmidtko, et al., 2010).

Understanding drivers of changes to marine oxygenation in the past is critical for understanding and predicting future change (Jaccard et al., 2014). Paleorecords provide an important archive to investigate temporal and spatial scales of changes to marine oxygenation. In general, warm intervals during the late Quaternary were associated with decreased global ocean oxygenation and cool intervals were associated with increased oxygenation (Cannariato & Kennett, 1999; Cardich et al., 2019; Erdem et al., 2019; Jaccard et al., 2014; Praetorius et al., 2015). The Holocene is an ideal epoch to investigate marine oxygenation because it has well documented intervals of oceanographic change and provides an opportunity to investigate ecological response to stress, including changes to temperature, oxygenation, carbon cycling and ocean circulation (Addison et al., 2017; Barron et al., 2003; Fisler & Hendy, 2008; Moffitt et al., 2015; Praetorius et al., 2015). Over millennial timescales, significant work along the California margin has documented paleoceanographic changes in coastal basins and within the bounds of the modern OMZ (Balestra et al., 2018; Cannariato & Kennett, 1999; Moffitt et al., 2014; Taylor et al., 2015). However, additional work is needed to constrain the timing and extent of oxygenation change below 1000 m, the relative impacts of surface processes and source waters on seafloor oxygenation, and how oxygenation at these depths responds to global and regional environmental change.

1.2 Southern California modern and paleoceanography

In the modern California Current eastern boundary upwelling system, an OMZ exists at approximately 500 – 1000 m water depth and is an important driver of ecosystem zonation, impacting species distributions in pelagic and seafloor communities (Helly & Levin, 2004; Stramma, Johnson, et al., 2010). The combination of high productivity, high export of organic matter, and age of water masses entering the

North Pacific at depth make this a particularly thick and laterally extensive OMZ (Bograd et al., 2008, 2019; Evans et al., 2020). The California Margin OMZ is expanding in intensity (decreasing dissolved oxygen), horizontal extent, and vertical thickness (shoaling) (Schmidtko et al., 2017; Stramma, Johnson, et al., 2010). Changes to the OMZ are caused by reductions in the oxygenation of source water and reduced ventilation due to surface warming and stratification (Bograd et al., 2008; Evans et al., 2020). Off the coast of California, dissolved oxygen decreased at a rate of up to 0.047 ml/L/year from 1984-2006 in the upper 500 m of the water column (Bograd et al., 2008, 2015). In the Southern California Current System, 81% of observed change in oxygenation in the upper 400 m of the water column from 1993-2018 can be attributed to changes in oxygenation of source waters (Evans et al., 2020).

In the modern system, Southern California Borderlands surface water flow is counterclockwise (Southern California Eddy), with the western margin dominated by the southward flowing California Current and the eastern margin driven by the northward-flowing California Countercurrent and Davidson Current. At depth, the California Undercurrent flows south to north and is comprised of a mix of Southern Component Intermediate Water from the eastern tropical Pacific and northerly sourced North Pacific Intermediate Water (Balestra et al., 2018; Bograd et al., 2019; Checkley & Barth, 2009; Stott et al., 2000; Talley, 1993). Offshore Southern California, a series of submarine basins, generally deepening from north to south, structure intermediate and deep-water flow (Berelson, 1991; Berelson & Stott, 2003). Oxygenation in basinal environments is impacted by the export of organic matter from overlying surface waters, advection of intermediate and deep waters that spill into the basin, and within basin processes, including sediment and pelagic biogeochemical cycles. By examining the environments of multiple silled basins, the effects of water advection can be separated from surface processes and the depths of significant biogeochemical change can be determined.

The California margin OMZ fluctuated throughout the Holocene (Balestra et al., 2018; Christensen et al., 1994; McGann, 2011; Moffitt et al., 2014; Palmer et al., 2020). Previous analyses of marine sediment cores from the Santa Barbara Basin (SBB) document intervals of hypoxia in the early Holocene (11.5-10 ka) followed by oscillations in the strength of the OMZ from 10-6 ka with several intervals of hypoxia (less than 0.5 ml L^{-1} [O_2]) and an increase in oxygenation in the last 6 ka within SBB, yet the OMZ persists throughout the Holocene (Moffitt et al., 2014; Ohkushi et al., 2013; Wang et al., 2020). In Santa Monica Basin (SMB), severe hypoxia (less than 0.3 ml L^{-1} [O_2]) was present from the start of the Holocene to 9 ka, and the mid to late Holocene (9-0 ka) had weaker hypoxia (0.3-1.5 ml L^{-1} [O_2]) than the early Holocene (Balestra et al., 2018). The modern OMZ, with oxygen levels at 0-1.5 ml L^{-1} [O_2], developed in the mid to late Holocene (by 6-4 ka) across the broader North Pacific (Addison et al., 2017;

McGann, 2011; Ohkushi et al., 2013; Praetorius et al., 2015). Over the past several centuries the SMB experienced variable degrees of dysoxia at interannual to interdecadal time scales (Christensen et al., 1994). These changes are attributable to variable biological carbon flux and respiration at depth (Berelson and Stott, 2003; Stott et al, 2000), underscoring how sensitive the shallow-silled basins are to small changes in biological productivity. Previous analysis of ecosystem responses (benthic foraminiferal and invertebrate) to oxygenation change through the Holocene from the SBB indicate that intervals within the Holocene exhibit distinct phases of ecosystems that do not repeat or overlap, as the oxygen minimum zone and carbon maximum zone fluctuate (Moffitt et al., 2015; Myhre et al., 2017).

Here, we utilize records from three offshore basins to constrain changes in ocean oxygenation through the Holocene and resultant impacts on benthic ecosystems. Silled basins provide a unique opportunity to examine both local changes within each basin and to compare oxygenation history across depths when records overlap temporally. Combining a series of silled basins allows for the examination of change through time at multiple water depths and sill depths to investigate the relative impact of surface processes and intermediate water changes in determining oxygenation at depth (Balestra et al., 2018; Moffitt et al., 2014; Wang et al., 2020).

1.3 Benthic foraminiferal assemblages as a metric of past oxygenation and organic matter export

Benthic foraminiferal assemblages are an effective and established metric to quantify past changes in marine oxygenation (Balestra et al., 2018; Belanger et al., 2020; Bernhard et al., 1997, 2003; Bernhard & Gupta, 1999; Cardich et al., 2015, 2019; Caulle et al., 2014; De & Gupta, 2010; Kaiho, 1994; Moffitt et al., 2014; Murgese & De Deckker, 2005; Ohkushi et al., 2013; Praetorius et al., 2015). Benthic foraminiferal assemblages are sensitive to small changes in oxygenation in the North Pacific, even in suboxic environments, not exclusively across large biological thresholds of anoxic or sulfidic conditions (Sharon et al., 2021). Multiple methodologies are used to interpret past environmental change from benthic foraminiferal assemblages, which we introduce and review below.

Quantifying absolute and relative abundance of benthic foraminiferal species is an established and foundational method; typically, studies quantify species downcore and interpret trends through time using observational or statistical approaches (e.g. Moffitt et al., 2014; McGann, 2011; Gardner et al., 1988). Studies of modern benthic foraminifera from multiple depositional environments and oxygenation regimes have identified oxygenation affinity of benthic foraminiferal species that can be used as indicator species of change through time; this method is most useful to reconstruct relative oxygenation or to

identify past oxygenation thresholds (e.g. Cannariato and Kennett, 1999; Palmer et al., 2020; Balestra et al., 2018; Bernhard and Gupta, 1999).

While these approaches provide relative oxygenation history, transfer functions are used to translate whole or partial benthic species assemblages into absolute oxygenation values (Behl & Kennett, 1996; Kaiho, 1994, 1999; McGann, 2011; Moffitt et al., 2014; Ohkushi et al., 2013; Sharon et al., 2021). Multi-species transfer functions including the Kaiho Benthic Foraminiferal Oxygenation Index, Schmiedl Dissolved Oxygen Index, and Behl Dissolved Oxygen Index are used to generate absolute values of past oxygenation by transforming the relative abundance of species into ml L^{-1} [O_2] (Kaiho, 1994; Ohkushi et al., 2013; Sharon et al., 2021). Transfer functions have typically been constructed using case studies from very low oxygen environments (such as Santa Barbara Basin) or by using the lowest known oxygen tolerance for a species; as such, this approach generates inherently conservative (lower) predictions of oxygenation, with the exception of the analysis by Sharon et al., 2021 which utilized multivariate statistical analysis to group species by oxygenation (Kaiho, 1994; Ohkushi et al., 2013; Sharon et al., 2021). Categorization of species into oxic, intermediate hypoxic, and anoxic environments used in multiple transfer functions and as indicator species varies by author (Bernhard et al., 1997; Bernhard & Gupta, 1999; Cannariato & Kennett, 1999; Kaiho, 1994; Moffitt et al., 2014; Palmer et al., 2020; Praetorius et al., 2015). Here we follow the convention: weakly suboxic/oxic ([O_2] >1.5 ml L^{-1}), intermediate hypoxic/suboxic ([O_2] 1.5-0.5 ml L^{-1}), and severe hypoxic/dysoxic ([O_2] <0.5 ml L^{-1}) (Moffitt et al., 2014; Palmer et al., 2020; Sharon et al., 2021; Tetard et al., 2021).

Recent work on paleoecological assemblages, including benthic foraminifera, utilizing analysis of diversity, richness, and multidimensional statistical analysis has expanded our breadth of understanding of how oxygenation impacts seafloor ecosystems (Belanger et al., 2020; Myhre et al., 2017; Sharon et al., 2021). Ecological analysis provides community-scale assessments of environmental change over time and often complements analysis of indicator taxa or transfer function calculations (Belanger et al., 2020; Myhre et al., 2017; Sharon et al., 2021). In addition to taxonomic evaluation of benthic foraminifera, studies are increasingly relying on morphometrics to assess past environments. These studies are predicated on morphological response or adaptation to oxygenation such as pore density, size, and shape (i.e., roundedness) and are used in both taxon-specific and taxon-independent analyses (Keating-Bitonti & Payne, 2016, 2018; Keating-Bitonti & Payne, 2017; Rathburn et al., 2018; Tetard et al., 2021). Typically, smaller, thin-walled, elongate species are indicative of low oxygen environments in which high-surface area to volume ratio is advantageous, to maximize oxygen absorption, while in well oxygenated

environments, larger, thick-walled and porcelaneous taxa with rounded shapes are dominant (Tetard et al., 2021).

Importantly though, oxygenation is not the only driver of benthic foraminiferal assemblages. Food availability, driven by the timing (pulsed vs. constant) and amount of export of organic matter, water depth, sediment grain size, and water temperature play an important role in structuring seafloor ecosystems, including benthic foraminiferal assemblages (Belanger et al., 2012, 2020; Kaiho, 1999; Venturelli et al., 2018). Here we employ stable isotope and benthic foraminiferal assemblage analyses to investigate cores from three silled basins in the Southern California Borderlands. By combining multiple approaches to assemblage analysis as listed above, we quantify changes in oxygenation below 1000 m, deconstruct surface vs. advective processes as drivers of change, and investigate changes in source waters. This multi-site, multi-faceted approach allows us to reconstruct change over time in each basin and to assess regional scale oxygenation history and environmental change in the Southern California Borderlands through the Holocene.

2 Methods

2.1 Study site

Cores were collected from three silled basins within the Southern California Borderlands (Figure 1). Tanner Basin is located west of the Channel Islands and is the farthest offshore. The basin has a sill depth of 1160 m and a bottom depth of approximately 1500 m (Figure 1). San Nicolas Basin is located south of San Nicolas Island and west of San Clemente Island. The basin has a sill depth of 1100 m and a bottom depth of approximately 1800 m (Figure 1). San Clemente Basin is located south of San Clemente Island and is the deepest site explored here. The basin has a sill depth of 1815 m and a bottom depth of approximately 1950 m (Figure 1). The water depth of each core was assessed at time of core collection and bottom depths of each basin were measured using GeoMapApp.

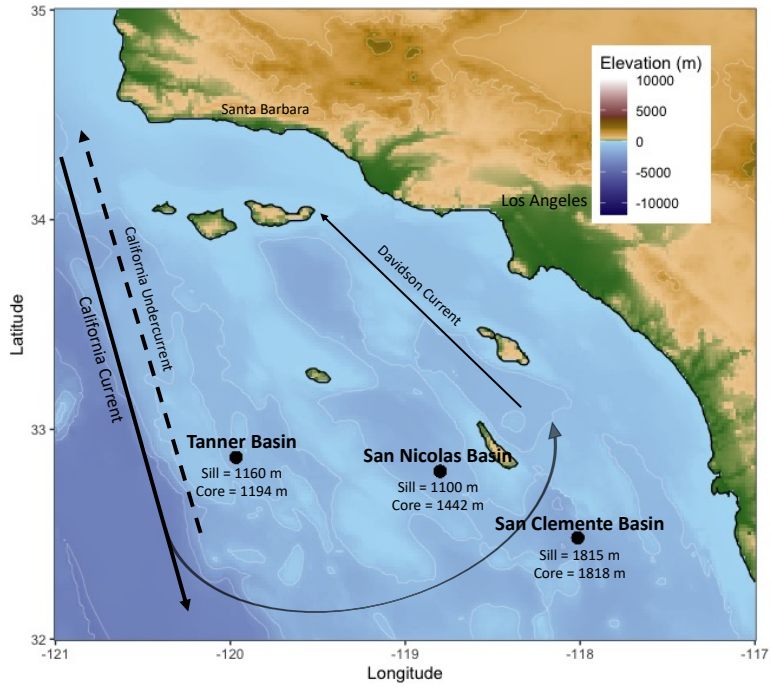

Figure 1: Map of the locations of the three cores used in this study. Schematic of current locations and directions included, solid lines indicate surface currents (California Current and Davidson Current), dashed line indicates subsurface current (California Undercurrent). The sill depth and core collection depth for each core is reported in meters.

2.2 Sediment cores

We investigate three piston cores collected from the Southern California Borderlands on the Maurice Ewing Cruise 9504 in May - June 1995: EW 9504-09PC from Tanner Basin at 1194 m water depth, EW 9504-08PC from San Nicolas Basin at 1442 m water depth, and EW 9504-05 from San Clemente Basin at 1818 m water depth. All cores have 10.16 cm inner diameter and were split and sampled at 2 cm intervals aboard the ship (initial volume of all samples was 162.15 cm^3). Sediments from the working half of the core were disaggregated in sodium hexametaphosphate washed over a 63 µm sieve (see Stott et al. 2000). Sediments were dried and stored in glass vials at the University of Southern California until they were processed for this study. The core from Tanner Basin (EW 9504-09PC) was examined from 0-40 cm at 2 cm intervals; intervals below 40 cm were not available for analysis (total of 19 intervals examined). The core from San Nicolas Basin (EW 9504-08PC) was examined at 2 cm intervals from 0-22 cm and every 6 cm from 24-64 cm (due to sample availability, total of 19 intervals examined). The core from San Clemente Basin (EW 9504-05) was examined at 2 cm intervals from 30-52 cm; intervals from 0-30 cm in EW9504-05 did not have sufficient foraminifera for robust analysis (see below) and were thus excluded from analysis (total of 11 intervals examined). Analysis was conducted at the resolution available to the

241 authors and all intervals with sufficient sediment volume and foraminifera (see below) were used in the
242 study.
243
244 **2.3 Radiocarbon dating and age model development**
245 Radiocarbon based age models were developed for each core using a combination of previously published
246 and newly generated planktic radiocarbon ages (Table S1, Figure S1). Five age dates within the Holocene
247 (1 San Clemente, 1 Tanner, 2 San Nicolas) were previously measured (Stott et al., 2000). These AMS ^{14}C
248 ages were completed using bulk planktonic foraminifera (weight ~3-5 mg) analyzed at the Lawrence
249 Livermore National Laboratory (Stott et al., 2000). Three additional radiocarbon dates (1 San Clemente, 2
250 Tanner, 1 San Nicolas) from bulk planktic foraminifera were analyzed in this study. All samples for
251 radiocarbon analysis were prepared by picking shell material from the >150 μm fraction, rinsing shells in
252 methanol, sonicating in methanol for 5-10 seconds, and rinsing twice with deionized water. Shells were
253 then dried in a $60^{O}C$ drying oven. Radiocarbon analysis was completed at the Lawrence Livermore
254 National Laboratory using $\delta^{13}C$ assumed values following the convention of Stuiver and Polach (1977).
255 The reported age is given in radiocarbon years using the Libby half-life of 5568 years. Accelerator mass
256 spectrometry ages were converted to calendar ages before present (BP) by calibration against the
257 Marine20 curve using the open-source software "R" package Bchron (Haslett & Parnell, 2008; Heaton et
258 al., 2020). Calibration included correction for reservoir ages for the Southern California Coast of 220.0 ±
259 40.0 years (Ingram & Southon, 1996; Stuiver & Polach, 1977). Age/depth models for each core were
260 generated using the Bayesian age-depth modeling functionality of Bchron (Table S1, Figure S1).
261
262 **2.4 Stable Isotope Analysis**
263 Stable isotope analyses from planktic and benthic foraminifera from EW9504-09 (Tanner Basin) were
264 conducted on *Globigerina bulloides* planktic foraminifera and *Cibicides mckannai* benthic foraminifera
265 from 0-40 cm at 2 cm intervals. Samples were prepared by picking from the >150 μm size fraction (2-5
266 individual *C. mckannai* per interval, 15-25 *G. bulloides* per interval) and cleaned using the same
267 methodology as above. Planktic foraminifera were analyzed at the UC Davis Stable Isotope Laboratory
268 and benthic foraminifera were analyzed at the UC Santa Cruz Stable Isotope Laboratory.
269
270 Planktic carbon and oxygen isotope samples were analyzed using a GasBench II system interfaced with a
271 Delta V Plus Isotope Ratio Mass Spectrometer at the UC Davis Stable Isotope Laboratory using standard
272 UCD-SM92 (-1.94 for $\delta^{18}O$ and 2.08‰ $\delta^{13}C$) (Ostermann 2000). Values for $\delta^{13}C$ and $\delta^{18}O$ are expressed
273 in per mil (‰) relative to Vienna Pee Dee Belemnite, and values are corrected for changes in linearity and
274 instrumental drift. Benthic carbon and oxygen isotope samples were analyzed at the UC Santa Cruz Stable

Isotope Laboratory by acid digestion using an individual vial acid drop Themo Scientific Kiel IV carbonate device interfaced to Thermo Scientific MAT 253 dual-inlet isotope ratio mass spectrometer. All samples were measured with several replicates of the externally calibrated Carrera Marble in-house standard reference material 'CM12' and the NBS-18 limestone international standard reference material. Values for $\delta^{13}C$ and $\delta^{18}O$ are expressed in per mil (‰) relative to Vienna Pee Dee Belemnite, and values are corrected for changes in linearity and instrumental drift. Data were combined with previously published records of planktic oxygen isotopes and benthic oxygen and carbon isotopes from the same core examined here (EW9504-09) to increase replicates in the late Holocene and to extend the record through the entire Holocene (Stott et al., 2000). As such, isotope records reflect analyses from three different laboratories. Instrument precision from all labs for $\delta^{13}C$ calcite was 0.05-0.06‰ and for $\delta^{18}O$ calcite was 0.06-0.10‰. Thus, we report the maximum uncertainty of 0.06‰ for $\delta^{13}C$ calcite and 0.10‰ for $\delta^{18}O$ calcite (Figure 3).

2.5 Benthic Foraminiferal Assemblages

Samples were dry sieved over a 150 µm sieve and picked for benthic foraminifera. Foraminifera greater than 150 µm have been documented to capture the range of environmental variability in paleoceanographic reconstructions as well as assemblages containing smaller foraminifera and the use of larger specimens results in reduced error in identification (Cannariato & Kennett, 1999; Caulle et al., 2014; Fenton et al., 2018; Palmer et al., 2020). Foraminifera in the size fraction below 150 µm were excluded from this analysis which may have excluded some smaller taxa or smaller individuals of the taxa identified here. Individual foraminifera were picked and identified from each interval to obtain >90 individuals per sample (Kemp et al., 2020), as sample sizes as low as 58 have been shown to have stable assemblages (Belanger et al., 2020; Forcino et al., 2015). The average number of individual foraminifera identified in each interval was 230, with a range of 90-665. Samples were mounted on micropaleontology slides using gum tragacanth at time of identification and are archived in the Ocean Climate Laboratory at the UC Davis Bodega Marine Laboratory. Cores were not laminated; thus, bioturbation is expected and may have had an averaging effect on assemblages.

2.6 Foraminiferal morphometrics

Morphometrics of benthic foraminifera, including length, width, and surface area were measured using ImageJ software. Length and width of each individual was measured to the longest and widest margins of the shell. Three species were selected for analysis to represent a gradient of oxygenation affinity: *Quinqueloculina* sp. is weakly suboxic/oxic and *B. spissa* and *U. peregrina* are categorized as suboxic (Table S2). Measurements of *Quinqueloculina* sp. and *B. spissa* were quantified in Tanner Basin at 2 cm

intervals from 0-40 cm, measurements of *Quinqueloculina* sp. and *U. peregrina* were quantified in San Clemente Basin at 2 cm intervals from 30-44 cm. From each interval, 3-30 individual shells of each species were measured (based on availability of taxa). Results of morphometric analysis were compared to morphometric data (collected using the same methodology) from five open coastal margin sites (300-1175m) near San Diego (see Palmer et al., 2020 for further explanation of the open margin study site, all morphometric data is available on Dryad, see Palmer et al., 2022).

2.7 Metazoan microfossil assemblages

In addition to picking and identifying benthic foraminifera, ostracods (Arthropoda - Ostracoda) and urchin spines (Echinodermata) were picked from the 150 μm sediment fraction at all intervals examined. Samples were mounted on micropaleontology slides using gum tragacanth at time of identification and are archived in the Ocean Climate Laboratory at the UC Davis Bodega Marine Laboratory. Due to low abundances, presence/absence is recorded, rather than relative abundance.

2.8 Benthic foraminiferal oxygenation index

Oxygenation was reconstructed using two modified benthic foraminiferal oxygenation indices: Behl and Schmiedl (Schmiedl et al., 2003; Sharon et al., 2021). Data were analyzed using both indices in order to compare the results; the Schmiedl Index uses diversity as a input, but does not include suboxic taxa, while the Behl Index does not include diversity, but includes oxic, suboxic, and weakly suboxic/dysoxic taxa (Ohkushi et al., 2013; Schmiedl et al., 2004). Using a combination of paleo and modern samples, Sharon et al., 2021 used detrended correspondence analysis (DCA) to expand the list of species that can be used as inputs to the Behl Index, thus allowing for its application in a broader range of seafloor environments (Sharon et al., 2021). Here we utilize the Behl dissolved oxygen index following Ohkushi et al., 2013, but expand the list of species included in the assessment following the work of Sharon et al., 2021. We further modified the list of species used in the Behl and Schmiedl indices by adding ten additional species using previously published oxygenation affiliations and morphometric or taxonomic similarities (Table S2). We included all species that made up at least 2% of the total foraminifera identified across all time intervals and cores examined. Oxygenation reconstructions were calculated using two equations:
Behl DO index = ((dysoxic % * 0.1) + (suboxic % * 0.5) + (weakly suboxic/oxic % * 1.5))/100 and
Schmiedl index = ((weakly suboxic/oxic %)/(weakly suboxic/oxic % + hypoxic %) + diversity (H`)) * 0.5 (Ohkushi et al., 2013).

2.9 Statistical analysis

Diversity of each interval was calculated using Shannon Index (H). Richness was calculated by tabulating the number of distinct species present in an interval. Non-metric multidimensional scaling (NMDS) ordination, using square root transformation of assemblage species counts and Bray-Curtis similarities and detrended correspondence analysis were conducted and compared (Figure S2, Table S3, S4). We used a single factor ANOVA to determine if there were significant differences among mean morphometrics (length, width, surface area), diversity between basins, diversity through time, and values of reconstructed vs. modern oxygenation. If the results of ANOVA were significant, we performed Tukey's Test to determine where differences in the means occurred. All statistical analyses were completed using the Vegan R package (nmds function, decorana function) or base R functions (tukeyHSD function and res.aov function) (Oksanen et al., 2013; R Core Team, 2021).

2.10 Modern oxygenation data

Modern oxygen data were sourced from the California Cooperative Oceanic Fisheries Investigations (CalCOFI) for the years 1949-2019. Data were included from all sites in the CalCOFI sampling grid bounded by -116° – -121° W longitude and 32° – 34.5° N latitude (Point Conception is northern boundary)) and depths 1000-2000 m to maximize data availability. Oxygenation was calculated using Winkler Titration of bottle samples at the Scripps Institution of Oceanography (Bograd et al., 2003; Bograd & Lynn, 2003). Flagged data from CalCOFI and property-property and time series analysis excluded 19 data points. The CalCOFI data set used here includes a total of 272 modern oxygen measurements.

3 Results

3.1 Age Model Development

Age models produced a median age and probability distribution (at a range of 95.0% uncertainty, 2σ) at each depth (Figure S1). Age model uncertainty is reported in Table S2. Coherence of age model within each core and between cores supports use of this age model (Figure S1). Mean sedimentation rates for the entire Holocene are similar for all three cores: Tanner has a mean sedimentation rate of 10.8 (± 1σ =5.3 cm/ka), San Nicolas has a mean sedimentation rate of 9.9 (± 1σ =1.8 cm/ka), and San Clemente has a mean sedimentation rate of 12.0 (± 1σ =4.8 cm/ka). Sedimentation rates reported here are similar to those observed offshore Central California through the Holocene (McGann, 2011). All following results are discussed as age in thousands of years before present (ka).

3.2 Benthic foraminiferal assemblages

Benthic foraminiferal assemblages were quantified down core for each core in which sufficient benthic foraminifera were present (Tanner Basin 0-40 cm at 2 cm intervals, San Nicolas Basin 0-22 cm at 2 cm intervals, 24-66 at 6 cm intervals, San Clemente Basin 30-54 cm at 2 cm intervals). The total number of species (richness) in each sample ranged from 15 to 24 (Figure S4) and species diversity (Shannon Index, H) ranged from 2.12 to 2.68, with a mean of 2.40 (± 1σ = 0.15) across all three basins (Figure S4). Species diversity (H) is significantly higher in Tanner Basin (mean=2.51, ± 1σ = 0.11), relative to San Nicolas Basin (mean=2.30, ± 1σ = 0.11) and San Clemente Basin (mean=2.37, ± 1σ = 0.10) (ANOVA, Tukey Test $p<0.05$) (Figure 3). Comparison of diversity through time in individual basins using 0.5 or 1 ka time bins shows that diversity (H) is not statistically different through time in Tanner, San Nicolas, and San Clemente basins (ANOVA, Tukey Test $p<0.05$ for all sites). Multivariate statistical analysis using nonmetric multidimensional scaling (NMDS) and detrended correspondence analysis (DCA) of down-core assemblages shows that, through time, assemblage similarity within sites exceeds similarity to assemblages at any other site (Figure S2). Comparison of results of DCA and NMDS with previously published benthic foraminiferal species categorization by oxygenation do not clearly indicate that oxygenation is the dominant factor in controlling species assemblage at the community level.

In Tanner Basin, the most common species (in descending order) are *B. spissa, G. subglobosa, H. soldanii, Quinqueloculina* sp., and *P. murrhina* (Figure 2). Species diversity (H) ranged from 2.32-2.68 with a mean of 2.51 (± 1σ = 0.11) (Figure 3). Benthic foraminiferal assemblage gradually changed from 5.5 – 1.9 ka; this shift is largely driven by a gradual increase in *Hansenisca soldanii* (previously *Gyroidina soldanii*) and decrease in *B. spissa* and *U. peregrina* (Figure 2). *G. subglobosa* and *Quinqueloculina* sp consistently make up 10-20% of the assemblage through time (Figure 2). In San Nicolas Basin, the most common species (in descending order) are *U. peregrina, E. pacifica, C. mckannai, B. spissa,* and *Uvigerina* sp (Figure 2). Species diversity (H) ranges from 2.12-2.56 with a mean of 2.30 (± 0.11) (Figure 3). The assemblage in San Nicolas Basin exhibits little change through time from 10.1-4.7 ka when *U. peregrina* makes up 15-45% of the assemblage. From 4.7-4.2 ka, there is a sharp decline in *U. peregrina* and a sharp increase in *C. mckannai* (Figure 2). From 4.0-1.9 ka, the trend reverses, and the assemblage is very similar to the assemblage from 10.1-4.7 ka. In San Clemente Basin, the most common species (in descending order) are *U. peregrina, C. mckannai, E. pacifica, Quinqueloculina* sp., and *Uvigerina* sp (Figure 2). Species diversity (H) ranges from 2.17-2.51 with a mean of 2.37 (± 0.10) (Figure 3). In San Clemente Basin, relative abundance of benthic foraminifera exhibits little change over time from 11.2-7.1 ka as shown by both individual species analysis and DCA (Figure S2).

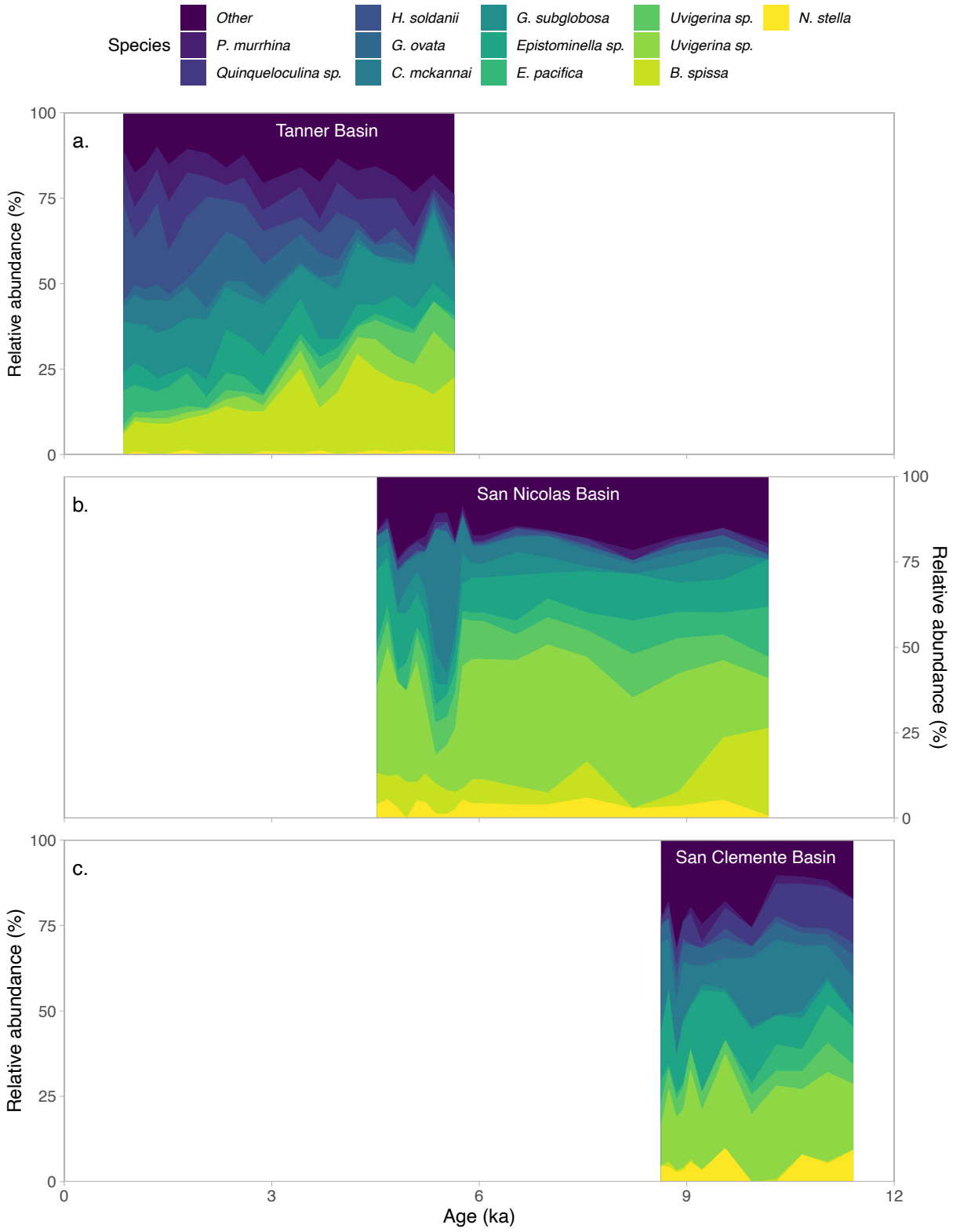

Figure 2: Relative abundance of benthic foraminifera vs. age in thousands of years before present for three cores examined here: Tanner (a.), San Nicolas (b.), and San Clemente (c.). Ten most abundant

species are shown; all other species grouped as "other." Each color represents a taxonomic group (species, genus, or other). See legend at top of plot for color of each. Taxa colors are ordered from dysoxic indicator taxa (yellow/bottom of plot) to oxic indicator taxa (blue/top of plot).

3.3 Shell morphometrics

Shell size was quantified to examine sub-lethal impacts of environmental change on benthic fauna. Shell size, measured as length, width, and surface area of three taxa (*U. peregrina, Quinqueloculina* sp., and *B. spissa*) was compared across the three cores examined here and to size data from a suite of cores from the San Diego Margin (Palmer et al., 2020). Shell size of *U. peregrina* is statistically significantly larger in coastal sites ($p<0.05$) relative to San Clemente basin (Figure S3a). Shell size of *B. spissa* is statistically significantly larger in coastal sites ($p<0.05$) relative to Tanner Basin (Figure S3a). Shell size of *B. spissa* and *Quinqueloculina* from Tanner Basin show relatively little variability through time (5.5-1.9 ka) (Figure S3b, c). As all metrics of shell size (length, width, and surface area) show the same trends, further discussion uses only shell surface area as a metric of whole shell size.

3.4 Reconstructed oxygenation using transfer functions

Reconstructed dissolved oxygen using the Behl Index ranges from 0.56-1.12 ml L^{-1} with a mean of 0.79 ml L^{-1} (Figure S4) and varies across basins: Tanner Basin mean is 0.86 ml L^{-1} and ranges from 0.59-1.12 ml L^{-1}, San Nicolas Basin mean is 0.67 ml L^{-1} and ranges from 0.56-1.02 ml L^{-1}, and San Clemente Basin mean is 0.84 ml L^{-1} and ranges from 0.68-0.96 ml L^{-1}. Reconstructed dissolved oxygen using the Schmiedl Index ranges from 1.36-1.81 ml L^{-1} for all three cores, with a mean of 1.62 ml L^{-1} (Figure S4). Schmiedl Index reconstructed oxygenation varies across basins: Tanner Basin mean is 1.73 ml L^{-1} and ranges from 1.59-1.81 ml L^{-1}, San Nicolas Basin mean is 1.50 ml L^{-1} and ranges from 1.36-1.66 ml L^{-1}, and San Clemente Basin mean is 1.60 ml L^{-1} and ranges from 1.48-1.71 ml L^{-1}. Importantly, the number of individual foraminifera identified did not impact the outcomes of the Behl or Schmiedl indices (Figure S4). Species richness is not correlated with outputs of the Behl Index, but is positively correlated with the Schmiedl Index (Figure S4).

3.5 Stable isotope record

Stable isotope records from Tanner Basin varied slightly through time (Figure 3). Analysis of planktic oxygen and carbon isotopes from *G. bulloides* yielded the following: $\delta^{13}C$ mean is -0.59 ($\pm 1\sigma = 0.25$), range is -0.92 to -0.05, $\delta^{18}O$ mean is 0.22 ($\pm 1\sigma = 0.31$), range is -0.15 to 1.08 (Figure 3). Analysis of benthic oxygen and carbon isotopes from *C. mckannai* yielded the following: $\delta^{13}C$ mean is -0.03 ($\pm 1\sigma$ =0.07), range is -0.13 to 0.10, $\delta^{18}O$ mean is 2.53 ($\pm 1\sigma = 0.17$), range is 2.29 to 2.73 (Figure 3).

3.6 Metazoan microfossil analysis

Urchin spines and ostracods were present in the Tanner Basin core, but do not present a coeval trend; urchins are present in 13 of 19 intervals, ostracods are present in 5 of 19 samples. Urchin spines and ostracods were scarce in sediments from San Nicolas Basin: urchin spines are present in 6 of 17 and ostracods are present in 2 of 17 intervals. Ostracods and urchin spines were nearly ubiquitous (present in every interval except one) in San Clemente Basin (Figure S5).

3.7 Modern oxygenation in the Southern California Borderlands

Modern oxygenation decreases linearly with depth from 1000 to 2000 m in this region, and ranges from 0.15-1.67 ml L^{-1} and has a mean of 0.78 ml L^{-1} across all depths (1000-2000m). Modern oxygenation in the 50 m above and below the Tanner Basin site (1144-1244 m) has a mean of 0.77 ± 0.18 ml L^{-1}. Modern oxygenation in the 50 m above and below the San Nicolas Basin site (1392-1492 m) has a mean of 0.88 ± 0.37 ml L^{-1}. Modern oxygenation in the 50 m above and below the San Nicolas Basin site (1392-1492 m) has a mean of 1.51 ± 0.09 ml L^{-1}.

	Tanner Basin		**San Nicolas Basin**		**San Clemente Basin**	
	Mean	Range	Mean	Range	Mean	Range
Behl Index reconstructed oxygen (ml L^{-1})	0.86	0.59-1.12	0.67	0.56-1.02	0.84	0.68-0.96
Schmiedl Index reconstructed oxygen (ml L^{-1})	1.73	1.59-1.81	1.50	1.36-1.66	1.60	1.48-1.71
Modern dissolved oxygen (ml L^{-1})	0.77	0.31-1.45	0.88	0.28-1.39	1.51	1.39-1.61

Table 1: Reconstructed and modern dissolved oxygen values for Tanner, San Nicolas, and San Clemente Basins. Modern oxygenation is from CalCOFI data from 50 m above and below the water depth of core collection for each basin.

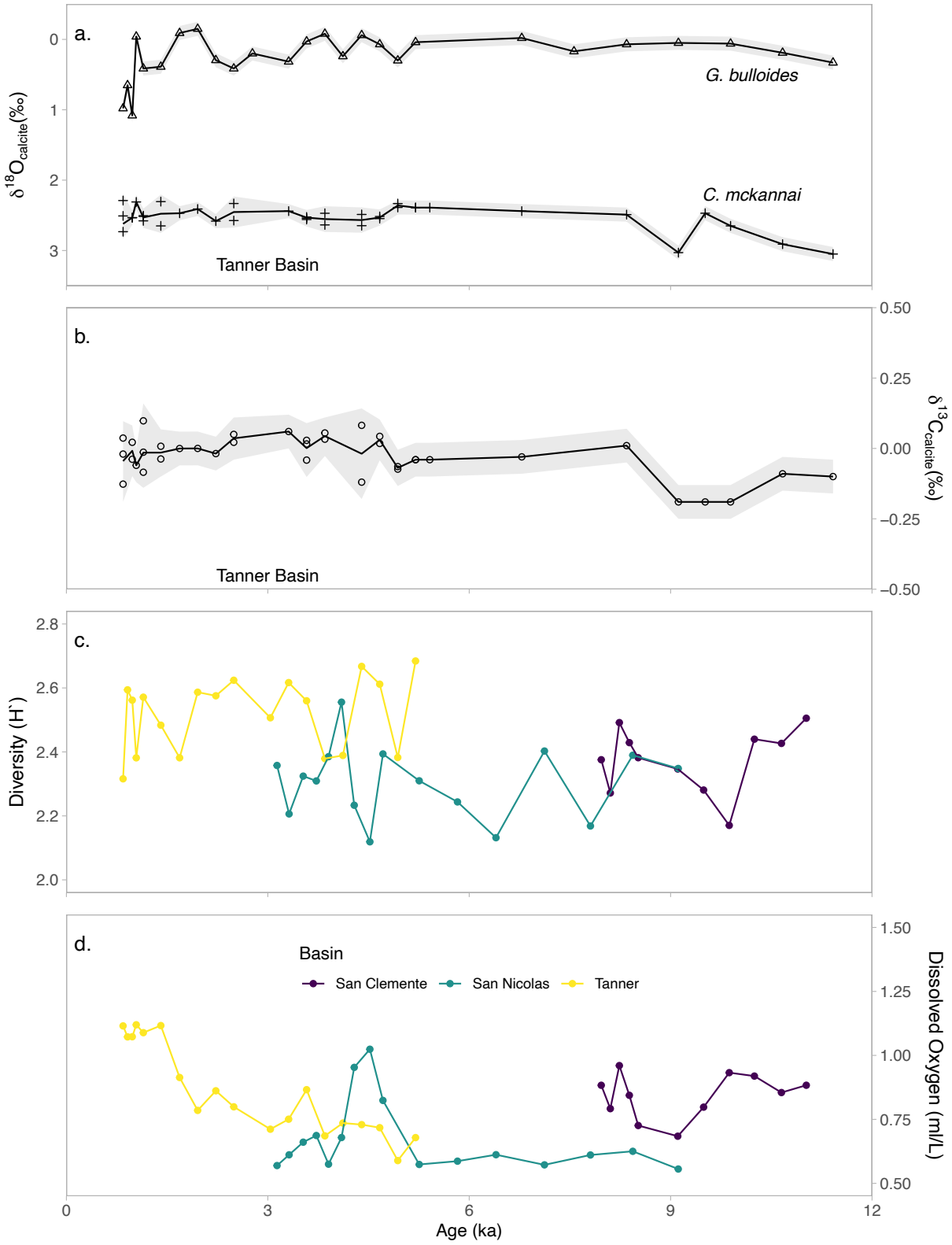
a.
G. bulloides
C. mckannai
Tanner Basin
δ18Ocalcite (‰)
0
1
2
3
b.
Tanner Basin
δ13Ccalcite (‰)
0.50
0.25
0.00
−0.25
−0.50
c.
Diversity (H')
2.8
2.6
2.4
2.2
2.0
d.
Basin
San Clemente
San Nicolas
Tanner
Dissolved Oxygen (ml/L)
1.50
1.25
1.00
0.75
0.50
0
3
6
9
12
Age (ka)

Figure 3: Stable isotope record from Tanner Basin (a., b.), benthic foraminiferal diversity (c.), and reconstructed oxygenation (d.) for all three sites using Behl Dissolved Oxygen Index. Oxygen isotopes of planktic foraminifera *G. bulloides* from this study and Stott et al., 2000 indicated as triangles (a.). Oxygen and carbon isotopes of benthic foraminifera *C. mckannai* from this study and Stott et al., 2000 indicated as + (b.). Analytical uncertainty for stable isotopes is shown as gray bar ($\delta^{13}C$ ±0.06‰ and $\delta^{18}O$ ±0.10‰). In the isotope figures, data from 3.8-0.8 ka includes both data from Stott et al., 2000 and this study, data from 11.4-3.8 ka is from Stott et al., 2000. For diversity and reconstructed dissolved oxygen yellow indicates Tanner, green indicates San Nicolas, and purple indicated San Clemente). Oxygen is reported in ml L^{-1}. **Discussion**

4.1 Paleo-oxygenation reconstruction

By analyzing the complete assemblage from each basin, we interpret a gradual shift in relative abundance of taxa in Tanner Basin, multi-centennial shifts in the assemblage at San Nicolas Basin, and stability in the assemblage in San Clemente Basin. Examining indicator taxa, we identify a decrease in suboxic taxon *B. spissa* and a decrease in *U. peregrina* coeval with an increase in oxic indicator *Hansenisca* sp. in Tanner Basin from 1.7 to 0.8 ka. In San Nicolas Basin, we observe a short period of divergence from the mean assemblage driven by an increase in the oxic-associated taxon *C. mckannai* and a sharp decline in *U. peregrina* from 4.7-4.3 ka. We observe little change over time in the relative abundance of these indicator taxa in San Clemente Basin. We do not identify a relationship between NMDS and DCA species scores and previously published categories of oxygenation indicating that oxygenation may not be the dominant factor in determining the full assemblage. Other parameters such as proximity to the margin of the OMZ, sediment grain size, and organic matter availability also play important roles in structuring foraminiferal diversity and assemblage (e.g., Bernhard et al., 1997; Sharon et al., 2021; Venturelli et al., 2018).

Reconstructed oxygen concentration differs between the two transfer functions compared here. Reconstructed dissolved oxygen using Behl Index for all three cores yields values (0.56-1.12 ml L^{-1}) within “intermediate hypoxia” as defined by Moffitt et al., and “suboxic” as defined by Cannariato and Kennett and Kaiho (Cannariato & Kennett, 1999; Kaiho, 1994; Moffitt et al., 2014). Reconstructed values using the Behl Index are similar to the range of modern values for bottom water oxygenation with notable exceptions discussed below (Figure 3d, 4). In comparison, the Schmiedl Index output is higher (1.36-1.81 ml L^{-1}) than the Behl Index by approximately 0.5 ml L^{-1} (Figure S4). We posit that this is due to the fact that diversity and oxygenation are not necessarily inversely correlated, particularly in intermediate hypoxic environments, yet the Schmiedl Index is based on diversity. Oxygenation plays a more dominant role in structuring diversity across biological thresholds (such as below 0.5 ml L-1 [O_2]) than across

oxygen gradients that do not cross biological thresholds (McGann, 2011; Palmer et al., 2020; Sharon et al., 2021; Venturelli et al., 2018). Additionally, the Schmiedl index only considers the end member groups: hypoxic and weakly suboxic/oxic, and does not include the relative abundance of suboxic taxa, taxa which may be important community members and oxygenation indicators at this water depth. Thus, we utilize the Behl Index to reconstruct absolute values of paleo-oxygenation (Figure 3).

4.2 Ecological and environmental change through the Holocene in the Southern California Borderlands

Geochemical and faunal records from Tanner, San Nicolas, and San Clemente Basins indicate environmental and ecological stability in water below 1000m through the Holocene in the Southern California Borderlands. Planktic $\delta^{18}O$ records from Tanner Basin indicate constant sea surface conditions (salinity/temperature) through most of the Holocene (11.75 – 2.3 ka) and a decrease in sea surface temperature or increase in salinity from 1.0-0.8 ka relative to the rest of the Holocene (Figure 3). Benthic $\delta^{18}O$ and $\delta^{13}C$ of the epibenthic foraminifera *C. makannai* exhibit little change through the Holocene (Figure 4). Reconstructed seafloor oxygenation using the Behl Index is within the range of intermediate hypoxia (0.5 – 1.5 ml L^{-1}) and are similar to the range of modern values for bottom water oxygenation with notable exceptions discussed below (Figure 3d, 4).

Ecological and environmental change over time as measured by diversity and multi-dimensional community metrics also indicate stability through the Holocene. Diversity varied little between basins and through time within each basin. Shannon Index of diversity (H) ranged from 2.12 to 2.68 across all sites and points in time, and diversity did not significantly change through time at any site across this interval (ANOVA, $p>0.05$) (Figure 3, S4). Results of NMDS and DCA show species assemblages are distinct in each basin; at any time point, assemblages are more similar to other time points from the same basin than to any other time point from an adjacent basin (Figure S2). This demonstrates that each basinal environment is unique and the analysis of benthic foraminifera as environmental indicators must consider local factors. We hypothesize that the stability in diversity and community-scale ecology indicates that environmental conditions were also relatively stable through this interval. This evidence aligns with results of oxygenation reconstruction from the Behl Index and stable isotope analysis (Figure 3).

Changes in benthic foraminifera morphology can reflect environmental variations that are missed by community-based analyses. Comparison of two species (*U. peregrina*, *B. spissa*) between basins (studied here) and open margin sediments (San Diego Margin, 300-1200 m water depth see Palmer et al., 2020) shows that both species are larger in the nearshore environment relative to offshore basins (Tanner, San

Clemente Basin, see Figure S3). At this scale, we interpret the size difference to be representative of higher relative organic matter input at coastal margin sites or warmer bottom water temperatures at shallower coastal margin sites in comparison to offshore basins (Keating-Bitonti & Payne, 2016, 2018). Importantly though, in comparison to changes between coastal margins and offshore basins, there is relatively little change in shell size of *Quinqueloculina* sp. (oxic indicator species) or *B. spissa* (suboxic indicator species) over time (5.4-0.8 ka) in Tanner Basin (Figure S3). Thus, benthic foraminiferal $\delta^{18}O$ and $\delta^{13}C$, reconstructed dissolved oxygen (Behl Index), community scale ecology, and morphology all indicate relative stability in environmental conditions at water depths 1194-1818 m through the studied time interval with few notable exceptions discussed below.

4.2.1 Ecological and environmental change through time in Tanner Basin

In Tanner Basin, the benthic foraminiferal assemblage shifts from more hypoxic taxa at 5.4-1.7 ka to more oxic associated taxa from 1.7-0.8 ka (Figures 2, 3). This shift is largely driven by the increase in *Hansenisca soldanii* (previously *Gyroidina soldanii*) and decrease in *B. spissa* and *U. peregrina* (Figure 2). *Hansenisca soldanii* has been documented in well oxygenated, oligotrophic, cold deep water with pulsed food supply (De & Gupta, 2010), and both *B. spissa* and *U. peregrina* are well documented indicators of low oxygen. Using the modified Behl Index, reconstructed oxygenation increases from 0.58 to 1.12 ml L^{-1} across this interval (Figure 3). Thus, we interpret this assemblage shift as an indication of a increase of approximately 0.4 ml L^{-1} in Tanner Basin occurring around 1.7 ka.

Downcore morphometric analysis shows that neither relative abundance nor surface area of *Quinqueloculina* sp. (an oxic indicator species) changes through time. Although *B. spissa* decreases in relative abundance from 5.4-0.8 ka, shell size (surface area) does not change through time (Figure S3). Stability in shell size concurrent with changes in relative abundance may indicate an interaction of factors including oxygen and organic matter influx in determining lethal vs. sublethal effects on *B. spissa*. Further, the lack of changes in shell size of *B. spissa* and *Quinqueloculina* across this interval may indicate a consistent supply of surface-exported organic matter, the main food resource for these benthic foraminifera. Ostracod and echinoderm presence are not correlated with increase in dissolved oxygen at this site (Figure S5). We hypothesize that the shift identified in the benthic foraminiferal assemblage is in response to a relatively small change in oxygenation (less than 1 ml L^{-1}) and does not represent fluctuations across biologically important thresholds for metazoan taxa, as dissolved oxygen was never below 0.4 ml L^{-1} (Figure 3).

When compared to modern CalCOFI data, reconstructed oxygenation (using the Behl Index) is within 1σ of modern mean oxygenation (Figure 4), except for the interval from 1.7 – 0.8 ka in which reconstructed oxygen is higher than modern by 0.3 ml L^{-1} (Figure 4). There is no significant difference (ANOVA, Tukey, p=0.51) between reconstructed oxygenation values (mean=0.86 ml L^{-1}) and all modern oxygenation values (mean=0.77 ml L-1) within waters 50 m above and below the Tanner Basin site (Figure 4). Combining assemblage, oxygenation index, and isotopic records of Tanner Basin, we identify increased dissolved oxygen in the basin from 1.7-0.8 ka relative to 5.4-1.7 ka that is not correlated with changes in either the oxygen or carbon isotope records and remains within the modern range of dissolved oxygen variability. The changes in Tanner Basin dissolved oxygen are minor when compared to changes in oxygenation in nearby more shallow basins within the OMZ (Balestra et al., 2018; Moffitt et al., 2014; Palmer et al., 2020; Wang et al., 2020).

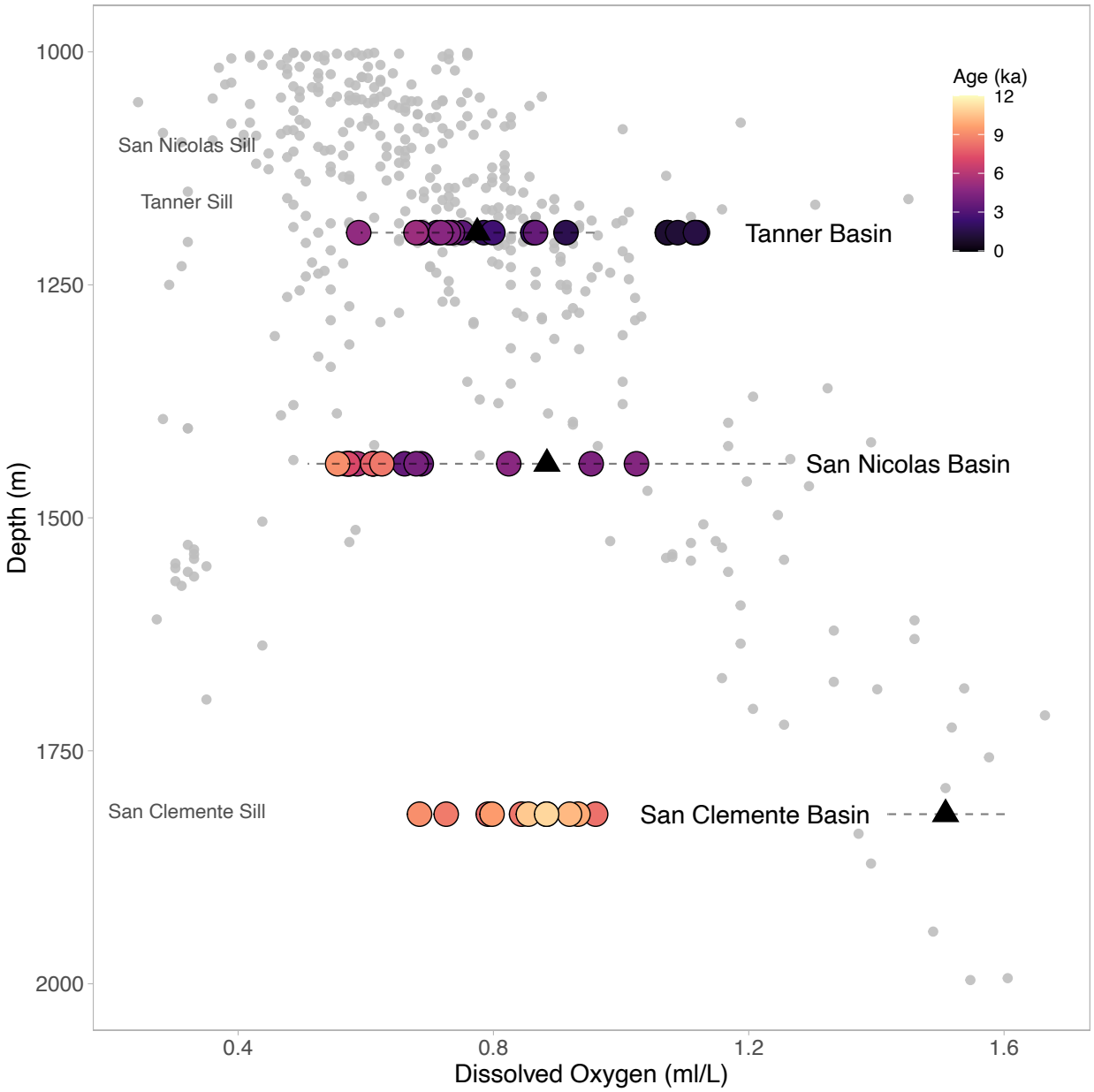

Figure 4: Reconstructed dissolved oxygen concentration (ml L^{-1}) from Tanner, San Nicolas, and San Clemente Basin (large dots colored by age) compared with modern dissolved oxygen concentration (ml L^{-1}) from CalCOFI bottle sampling (1986-2019) (shown in small gray dots). Depth of sill of each basin is labeled. Black triangles show mean modern dissolved oxygen concentration from 50 m above and below each site and dashed gray line shows 1σ range in modern dissolved oxygen concentration from 50 m above and below each site.

4.2.2 Ecological and environmental change through time in San Nicolas Basin

In San Nicolas Basin, low oxygen-associated benthic foraminiferal taxa dominate from 9.8 to 4.7 ka. A short period of anomalous assemblage driven by an increase in *C. mckannai,* an oxic-associated taxon, and a sharp decline in *U. peregrina*, an intermediate hypoxia-associated taxon, occurs at 4.7-4.3 ka and is interpreted as an interval of increased oxygenation. Using the modified Behl Index, reconstructed oxygenation increases from 0.59 ml L^{-1} before the interval to a maximum of 1.03 ml L^{-1} during the oxygenation interval (Figure 3). Oxygenation returned to pre-event levels of dissolved oxygen after 4.3 ka and pre and post event assemblages are similar, indicating an absence of a legacy effect of the event on the community (Figure 2). Metazoan invertebrate microfossils (ostracods and urchin spines) are scarce in this core and changes in presence/absence of metazoans do not correlate with shifts in benthic foraminiferal assemblages (Figure S5). Modern studies of circulation in San Nicolas Basin indicate that residence time for bottom waters in the basin are 9 ± 2 months (Berelson, 1991). As such, we hypothesize that the assemblage response recorded here represents persistent oxygenation or repeated ventilation on a decadal-to centennial scale, rather than a single episode of ventilation. Yet, the absolute change in oxygenation is relatively minor and still within a threshold of intermediate hypoxia and within the range of modern values (Figure 3, 4).

When compared to modern CalCOFI data, reconstructed oxygenation in San Nicolas Basin is slightly lower than modern mean dissolved oxygen yet remains within 1σ of the modern mean at all points throughout the Holocene (Figure 4). Reconstructed oxygenation (mean=0.67 ml L^{-1}) is statistically lower than modern oxygenation from waters 50 m above and below the depth of the San Nicolas site (ANOVA, Tukey $p<0.05$) (Figure 4). Further, the variance in reconstructed dissolved oxygen is similar to variance in modern oxygenation at the sill depth of San Nicolas Basin (1100m, see Figure 4). The scale of change in reconstructed dissolved oxygen, relative abundance of species, and species diversity in San Nicolas Basin across this interval of change is minor when compared to intervals of change in nearby basins across the deglacial and in comparison to Holocene changes within basins that experienced shifts between anoxic and oxic conditions, such as the Macoma Event in the Santa Barbara Basin (Balestra et al., 2018; Cannariato & Kennett, 1999; Moffitt et al., 2015; Praetorius et al., 2015; Schimmelmann et al., 2013).

4.2.3 Ecological and environmental change through time in San Clemente Basin

Environmental conditions remained relatively constant in San Clemente Basin from 11.0-8.0 ka as demonstrated by the lack of variability in the benthic foraminiferal assemblages. Species diversity does not change significantly through time (Figure 3, S4). Reconstructed oxygenation from the modified Behl Index ranges from 0.67 to 0.96 ml L^{-1} across this interval; this variability is reduced relative to Tanner and San Nicolas Basins (Figure 3). The assemblage at this depth is distinct from coastal margin environments

and other, shallower basins (Balestra et al., 2018; Moffitt et al., 2014; Palmer et al., 2020). Ostracods and urchin spines are present in every interval (except one) examined here, indicating a well-oxygenated seafloor environment that supported metazoan life and motile organisms (Figure S5) (Moffitt et al., 2015). Ecological differences between the shallow sill basins (San Nicolas and Tanner) vs. the deep sill basin (San Clemente) documented here are mirrored in previously documented seafloor metazoan assemblages (France, 1994). We hypothesize that at 1815 m water depth, this site was not impacted by changes in the oxygen minimum zone during the Holocene and that intermediate and deep water reaching this site had a consistent source from 11.0-8.0 ka.

In comparison to modern CalCOFI data, reconstructed dissolved oxygen (mean=0.84 ml L^{-1}) in the early and mid-Holocene is statistically lower than modern dissolved oxygen (mean=1.50 ml L^{-1}) within 50 m above and below the depth of the San Clemente Site ($p<0.05$) (Figure 4). We propose three potentially overlapping hypotheses for this difference. First, this may be an artifact of categorizations of some species used in the Behl Index that use lowest known thresholds of oxygenation and thus may predict the minima of dissolved oxygen concentrations. Second, in the early Holocene, sea level was lower than modern (by approximately 70 m), thus, the sites sampled here may have been less well oxygenated simply due to being at a shallower depth, but this would not entirely explain the difference from modern (Figure 4) (Fleming et al., 1998; Moffitt et al., 2014). Finally, the preformed oxygenation of the incoming water masses may have been lower than modern, a pattern that is reflected in Santa Monica and Santa Barbara Basins at this time (Balestra et al., 2018; Wang et al., 2020).

4.3 Environmental stability in Southern California Borderlands through the Holocene and comparison to modern ocean conditions

Environmental conditions in Tanner, San Nicolas, and San Clemente Basins remained relatively stable across the time intervals examined. In the early to mid-Holocene (11.0-4.7 ka), seafloor oxygenation and environmental conditions more broadly below 1400 m were stable in the Southern CA Borderlands, evidenced by stability in assemblage records from San Clemente Basin (1815 m) and San Nicolas Basin (1442 m), and was likely driven by consistent source and composition of intermediate waters. Benthic foraminiferal assemblage records from the Santa Lucia Slope (ODP 1017, 955 m) offshore Point Conception indicate a stable suboxic environment (reconstructed [O_2] 1.5-0.5 ml L^{-1}) through the early and mid-Holocene and are similar in taxonomic composition to the records presented here from San Nicolas and San Clemente Basins (Cannariato & Kennett, 1999; Sharon & Belanger, 2022). Synchrony in stability and assemblages across San Nicolas Basin (1442 m), San Clemente Basin (1818 m), and the Santa Lucia Slope (955 m) contrasts with evidence of fluctuations in age of North Pacific Intermediate

Water entering SBB (as recorded by benthic-planktic radiocarbon age differences) at 9 ka (Roark et al., 2003), expansion of the OMZ in SBB in the early Holocene (Wang et al., 2020), and a turning point from hypoxic to suboxic conditions at 9 ka in Santa Monica Basin (indicated by benthic foraminiferal assemblages and geochemical records) (Balestra et al., 2018). Differences in oxygenation between sites may be explained by differences across water depth; we propose that changes in the source and strength of NPIW impacted sites at 400-1000m water depth (SBB, SMB) (Balestra et al., 2018; Roark et al., 2003; Wang et al., 2020), but had less of an effect on the water column below 1000 m. Similar patterns of stable suboxic conditions below the depth of the OMZ and variability in dissolved oxygen at shallower, OMZ-impacted depths through the Holocene were observed further north, offshore British Columbia, and have been attributed to changes in the strength of NPIW (Sharon & Belanger, 2022). In the mid to late Holocene, San Nicolas Basin experienced a multi-centennial oxygenation interval from 4.7-4.3 ka and oxygenation increased in Tanner Basin beginning at 1.0 ka, yet all changes were within 1 ml L^{-1} [O_2] . Drivers of oxygenation in each basin may have been due to "indirect" ventilation through diffusion of dissolved oxygen from overlying waters, rather than "direct" ventilation due to advection (Talley, 1993), a change in oxygenation of source waters, or basinal processes related to the shape, depth, and overlying surface water productivity in each basin.

Although oxygenation does vary across the Holocene in Tanner, San Nicolas, and San Clemente basins, all variability was within 1 ml L^{-1} [O_2] and does not cross critical biological thresholds below 0.5 ml L^{-1} or above 1.5 ml L^{-1} in any basin. As such, variability in oxygenation and ventilation of San Nicolas, Tanner, and San Clemente basins is reduced relative to shallower sites, including Santa Barbara Basin and Santa Monica Basin, across the entire Holocene (Balestra et al., 2018; Moffitt et al., 2014; Ohkushi et al., 2013). Additionally, Holocene-scale oxygenation changes (presented here) are reduced relative to glacial/interglacial changes in oxygenation in the basins examined here and in the nearby Santa Lucia Slope (Cannariato & Kennett, 1999; Stott et al., 2000). This indicates that Holocene-scale climate changes driving oxygenation change shallower than 1000 m are not impacting waters below 1000 m and that climate changes within the Holocene do not significantly impact oxygenation below 1000 m, despite changes in the intensity and extent of the OMZ shallower than 1000 m. As such, we hypothesize that deoxygenation due to anthropogenic climate change will also have a greater impact on the water column above 1000 m, relative to below 1000m.

Direct comparison of reconstructed dissolved oxygen with modern measured dissolved oxygen indicates that the variance across millennia is similar to decadal-scale variance in the modern ocean (Figure 4). Variance in dissolved oxygen occurring on centennial to millennial timescales does not exceed the

690 variance observed in this modern ocean, indicating stability in intermediate waters and oxygenation below
691 1100 m in the Southern California Borderlands. We hypothesize that if there are significant changes to
692 oxygenation below 1000m due to anthropogenic climate change, these changes may have large impacts
693 on benthic ecosystems as they have not experienced significant changes in dissolved oxygen over the last
694 11 ka.
695
696 **5 Conclusion**
697 Reconstruction of past oxygenation using analysis of benthic microfaunal communities (foraminiferal and
698 metazoan) is optimized by combining multiple approaches including analysis of indicator taxa,
699 reconstruction of oxygenation using multi-taxa indices, and community scale-analysis such as
700 multidimensional analysis and diversity. Here we demonstrate the utility of combined approaches, and we
701 expand the use of the Behl Index for paleo-oxygenation reconstruction. Analysis of benthic foraminiferal
702 assemblages from three silled basins (Tanner, San Nicolas, San Clemente) in the Southern California
703 Borderlands combined with benthic and planktic stable isotope analysis from Tanner Basin show largely
704 stable oxygenation except for a gradual increase (approximately 0.4 ml L^{-1} [O_2]) in oxygenation in Tanner
705 Basin occurring at 1.7 ka and multi-centennial variability in oxygenation (approximately 0.5 ml L^{-1} [O_2])
706 in San Nicolas Basin. The seafloor environment is stable in San Clemente Basin from 11.0-8.0 ka, yet
707 reconstructed oxygenation is lower than modern at this site. Holocene scale climate changes did not drive
708 significant changes (> 1 ml L^{-1}) in marine oxygenation below 1000 m in the Southern California
709 Borderlands. In the context of modern oxygenation changes, findings from this analysis show that
710 seafloor oxygenation of the Southern California Borderlands through the Holocene below 1000 m
711 remained relatively stable and variance in oxygenation across millennia is similar to decadal-scale
712 variance in the modern ocean. As such, we expect that future changes to marine oxygenation will be
713 greater at depths above 1000 m relative to deeper waters and note that if anthropogenic climate change
714 induced changes in oxygenation do cause shifts in dissolved oxygen greater than > 1 ml L^{-1} below 1000
715 m, it will represent a divergence from scales of variability over the last 11 ka.
716

Acknowledgements

The authors declare no conflicts of interest. We acknowledge funding for this project provided through National Science Foundation Grant OCE 1832812 to TMH and PDR and the University of California, Davis Dissertation Year Grant and the University of California, Davis Earth and Planetary Sciences Durrell Fund Research Award. We thank Sarah Merolla and Kimberly Bowman for their support with sample preparation and processing. We thank Robin Trayler for his support and advice in developing the age model. We also thank Sharon for their assistance in multivariate statistics. We acknowledge three helpful reviewers whose input significantly improved this paper.

Open Research

The benthic foraminiferal assemblage data, radiocarbon age model data, carbon and oxygen stable isotope data, and morphometric data used for environmental reconstruction in the study are available at Dryad via Palmer et al. (2022).

731 **References**

732 Addison, J. A., Barron, J., Finney, B., Kusler, J., Bukry, D., Heusser, L. E., & Alexander, C. R. (2017). A
733 Holocene record of ocean productivity and upwelling from the northern California continental
734 slope. *Quaternary International*.

735 Balestra, B., Krupinski, N. B. Q., Erohina, T., Fessenden-Rahn, J., Rahn, T., & Paytan, A. (2018).
736 Bottom-water oxygenation and environmental change in Santa Monica Basin, Southern
737 California during the last 23 kyr. *Palaeogeography, Palaeoclimatology, Palaeoecology*, *490*, 17–
738 37.

739 Barron, J. A., Heusser, L., Herbert, T., & Lyle, M. (2003). High-resolution climatic evolution of coastal
740 northern California during the past 16,000 years. *Paleoceanography*, *18*(1).

741 Behl, R. J., & Kennett, J. P. (1996). Brief interstadial events in the Santa Barbara basin, NE Pacific,
742 during the past 60 kyr. *Nature*, *379*(6562), 243–246. https://doi.org/DOI 10.1038/379243a0

743 Belanger, C. L., Jablonski, D., Roy, K., Berke, S. K., Krug, A. Z., & Valentine, J. W. (2012). Global
744 environmental predictors of benthic marine biogeographic structure. *Proceedings of the National*
745 *Academy of Sciences*, *109*(35), 14046–14051. https://doi.org/10.1073/pnas.1212381109

746 Belanger, C. L., Sharon, Du, J., Payne, C. R., & Mix, A. C. (2020). North Pacific deep-sea ecosystem
747 responses reflect post-glacial switch to pulsed export productivity, deoxygenation, and
748 destratification. *Deep Sea Research Part I: Oceanographic Research Papers*, *164*, 103341.
749 https://doi.org/10.1016/j.dsr.2020.103341

750 Berelson, W. M. (1991). The flushing of two deep-sea basins, southern California borderland. *Limnology*
751 *and Oceanography*, *36*(6), 1150–1166. https://doi.org/10.4319/lo.1991.36.6.1150

752 Berelson, W. M., & Stott, L. D. (2003). Productivity and organic carbon rain to the California margin
753 seafloor: Modern and paleoceanographic perspectives. *Paleoceanography*, *18*(1), 2-1-2–15.
754 https://doi.org/10.1029/2001PA000672

755 Bernhard, J. M., & Gupta, B. K. S. (1999). Foraminifera of oxygen-depleted environments. In *Modern*
756 *foraminifera* (pp. 201–216). Springer.

757 Bernhard, J. M., Sen Gupta, B. K., & Borne, P. F. (1997). Benthic foraminiferal proxy to estimate dysoxic
758 bottom-water oxygen concentrations; Santa Barbara Basin, US Pacific continental margin. *The*
759 *Journal of Foraminiferal Research*, *27*(4), 301–310.
760 Bernhard, J. M., Visscher, P. T., & Bowser, S. S. (2003). Submillimeter life positions of bacteria, protists,
761 and metazoans in laminated sediments of the Santa Barbara Basin. *Limnology and*
762 *Oceanography*, *48*(2), 813–828.
763 Bograd, S. J., Buil, M. P., Lorenzo, E. D., Castro, C. G., Schroeder, I. D., Goericke, R., Anderson, C. R.,
764 Benitez-Nelson, C., & Whitney, F. A. (2015). Changes in source waters to the Southern
765 California Bight. *Deep Sea Research Part II: Topical Studies in Oceanography*, *112*, 42–52.
766 https://doi.org/10.1016/j.dsr2.2014.04.009
767 Bograd, S. J., Castro, C. G., Di Lorenzo, E., Palacios, D. M., Bailey, H., Gilly, W., & Chavez, F. P.
768 (2008). Oxygen declines and the shoaling of the hypoxic boundary in the California Current.
769 *Geophysical Research Letters*, *35*(12). https://doi.org/Artn L12607 10.1029/2008gl034185
770 Bograd, S. J., Checkley, D. A., & Wooster, W. S. (2003). CalCOFI: A half century of physical, chemical,
771 and biological research in the California Current System. *Deep Sea Research Part II: Topical*
772 *Studies in Oceanography*, *50*(14), 2349–2353. https://doi.org/10.1016/S0967-0645(03)00122-X
773 Bograd, S. J., & Lynn, R. J. (2003). Long-term variability in the Southern California Current System.
774 *Deep Sea Research Part II: Topical Studies in Oceanography*, *50*(14), 2355–2370.
775 https://doi.org/10.1016/S0967-0645(03)00131-0
776 Bograd, S. J., Schroeder, I. D., & Jacox, M. G. (2019). A water mass history of the Southern California
777 current system. *Geophysical Research Letters*, *46*(12), 6690–6698.
778 https://doi.org/10.1029/2019GL082685
779 Breitburg, D., Levin, L. A., Oschlies, A., Gregoire, M., Chavez, F. P., Conley, D. J., Garcon, V., Gilbert,
780 D., Gutierrez, D., Isensee, K., Jacinto, G. S., Limburg, K. E., Montes, I., Naqvi, S. W. A., Pitcher,
781 G. C., Rabalais, N. N., Roman, M. R., Rose, K. A., Seibel, B. A., … Zhang, J. (2018). Declining

oxygen in the global ocean and coastal waters. *Science*, *359*(6371), 46-+. https://doi.org/10.1126/science.aam7240

Cannariato, K. G., & Kennett, J. P. (1999). Climatically related millennial-scale fluctuations in strength of California margin oxygen-minimum zone during the past 60 k.y. *Geology*, *27*(11), 975–978. https://doi.org/Doi 10.1130/0091-7613(1999)027<0975:Crmsfi>2.3.Co;2

Cardich, J., Gutiérrez, D., Romero, D., Pérez, A., Quipúzcoa, L., Marquina, R., Yupanqui, W., Solís, J., Carhuapoma, W., Sifeddine, A., & Rathburn, A. (2015). Calcareous benthic foraminifera from the upper central Peruvian margin: Control of the assemblage by pore water redox and sedimentary organic matter. *Marine Ecology Progress Series*, *535*, 63–87. https://doi.org/10.3354/meps11409

Cardich, J., Sifeddine, A., Salvatteci, R., Romero, D., Briceño-Zuluaga, F., Graco, M., Anculle, T., Almeida, C., & Gutiérrez, D. (2019). Multidecadal Changes in Marine Subsurface Oxygenation Off Central Peru During the Last ca. 170 Years. *Frontiers in Marine Science*, *6*. https://doi.org/10.3389/fmars.2019.00270

Caulle, C., Koho, K. A., Mojtahid, M., Reichart, G. J., & Jorissen, F. J. (2014). Live (Rose Bengal stained) foraminiferal faunas from the northern Arabian Sea: Faunal succession within and below the OMZ. *Biogeosciences*, *11*(4), 1155–1175. https://doi.org/10.5194/bg-11-1155-2014

Checkley, D. M., & Barth, J. A. (2009). Patterns and processes in the California Current System. *Progress in Oceanography*, *83*(1–4), 49–64. https://doi.org/10.1016/j.pocean.2009.07.028

Christensen, C. J., Gorsline, D. S., Hammond, D. E., & Lund, S. P. (1994). Non-annual laminations and expansion of anoxic basin-floor conditions in Santa Monica Basin, California Borderland, over the past four centuries. *Marine Geology*, *116*(3–4), 399–418.

De, S., & Gupta, A. K. (2010). Deep-sea faunal provinces and their inferred environments in the Indian Ocean based on distribution of Recent benthic foraminifera. *Palaeogeography, Palaeoclimatology, Palaeoecology*, *291*(3), 429–442. https://doi.org/10.1016/j.palaeo.2010.03.012

808 Erdem, Z., Schönfeld, J., Rathburn, A. E., Perez, M.-E., Cardich, J., & Glock, N. (2019). Bottom-water
809 deoxygenation at the Peruvian Margin during the last deglaciation recorded by benthic
810 foraminifera. *Biogeosciences Discussions*. https://orcid.org/0000-0002-5509-8733
811 Evans, N., Schroeder, I. D., Buil, M. P., Jacox, M. G., & Bograd, S. J. (2020). Drivers of Subsurface
812 Deoxygenation in the Southern California Current System. *Geophysical Research Letters*, *47*(21),
813 e2020GL089274. https://doi.org/10.1029/2020GL089274
814 Fenton, I. S., Baranowski, U., Boscolo-Galazzo, F., Cheales, H., Fox, L., King, D. J., Larkin, C., Latas,
815 M., Liebrand, D., Miller, C. G., Nilsson-Kerr, K., Piga, E., Pugh, H., Remmelzwaal, S., Roseby,
816 Z. A., Smith, Y. M., Stukins, S., Taylor, B., Woodhouse, A., … Purvis, A. (2018). Factors
817 affecting consistency and accuracy in identifying modern macroperforate planktonic foraminifera.
818 *Journal of Micropalaeontology*, *37*(2), 431–443. https://doi.org/10.5194/jm-37-431-2018
819 Fisler, J., & Hendy, I. L. (2008). California Current System response to late Holocene climate cooling in
820 southern California. *Geophysical Research Letters*, *35*(9). https://doi.org/Artn L09702
821 10.1029/2008gl033902
822 Fleming, K., Johnston, P., Zwartz, D., Yokoyama, Y., Lambeck, K., & Chappell, J. (1998). Refining the
823 eustatic sea-level curve since the Last Glacial Maximum using far- and intermediate-field sites.
824 *Earth and Planetary Science Letters*, *163*(1), 327–342. https://doi.org/10.1016/S0012-
825 821X(98)00198-8
826 Forcino, F. L., Leighton, L. R., Twerdy, P., & Cahill, J. F. (2015). Reexamining Sample Size
827 Requirements for Multivariate, Abundance-Based Community Research: When Resources are
828 Limited, the Research Does Not Have to Be. *PLOS ONE*, *10*(6), e0128379.
829 https://doi.org/10.1371/journal.pone.0128379
830 France, S. C. (1994). Genetic population structure and gene flow among deep-sea
831 amphipods,Abyssorchomene spp., from six California Continental Borderland basins. *Marine*
832 *Biology*, *118*(1), 67–77. https://doi.org/10.1007/BF00699220

833 Gardner, J. V., Heusser, L. E., Quinterno, P. J., Stone, S. M., Barron, J. A., & Poore, R. Z. (1988). Clear
834 Lake record vs. The adjacent marine record; A correlation of their past 20,000 years of
835 paleoclimatic and paleoceanographic responses. In *Geological Society of America Special Papers*
836 (Vol. 214, pp. 171–182). Geological Society of America. https://doi.org/10.1130/SPE214-p171
837 Haslett, J., & Parnell, A. (2008). A simple monotone process with application to radiocarbon-dated depth
838 chronologies. *Journal of the Royal Statistical Society: Series C (Applied Statistics)*, *57*(4), 399–
839 418. https://doi.org/10.1111/j.1467-9876.2008.00623.x
840 Heaton, T. J., Köhler, P., Butzin, M., Bard, E., Reimer, R. W., Austin, W. E. N., Ramsey, C. B., Grootes,
841 P. M., Hughen, K. A., Kromer, B., Reimer, P. J., Adkins, J., Burke, A., Cook, M. S., Olsen, J., &
842 Skinner, L. C. (2020). Marine20—The Marine Radiocarbon Age Calibration Curve (0–55,000 cal
843 BP). *Radiocarbon*, *62*(4), 779–820. https://doi.org/10.1017/RDC.2020.68
844 Helly, J. J., & Levin, L. A. (2004). Global distribution of naturally occurring marine hypoxia on
845 continental margins. *Deep-Sea Research Part I-Oceanographic Research Papers*, *51*(9), 1159–
846 1168. https://doi.org/10.1016/j.dsr.2004.03.009
847 Ingram, B. L., & Southon, J. R. (1996). Reservoir ages in eastern Pacific coastal and estuarine waters.
848 *Radiocarbon*, *38*(3), 573–582.
849 Jaccard, S. L., Galbraith, E. D., Frolicher, T. L., & Gruber, N. (2014). Ocean (De)Oxygenation across the
850 Last Deglaciation Insights for the Future. *Oceanography*, *27*(1), 26–35.
851 Kaiho, K. (1994). Benthic Foraminiferal Dissolved-Oxygen Index and Dissolved-Oxygen Levels in the
852 Modern Ocean. *Geology*, *22*(8), 719–722. https://doi.org/Doi 10.1130/0091-
853 7613(1994)022<0719:Bfdoia>2.3.Co;2
854 Kaiho, K. (1999). Effect of organic carbon flux and dissolved oxygen on the benthic foraminiferal oxygen
855 index (BFOI). *Marine Micropaleontology*, *37*(1), 67–76. https://doi.org/Doi 10.1016/S0377-
856 8398(99)00008-0
857 Keating-Bitonti, C. R., & Payne, J. L. (2016). Physicochemical controls on biogeographic variation of
858 benthic foraminiferal test size and shape. *Paleobiology*, *42*(4), 595–611.

859 Keating-Bitonti, C. R., & Payne, J. L. (2017). Ecophenotypic responses of benthic foraminifera to oxygen
860 availability along an oxygen gradient in the California Borderland. *Marine Ecology*, *38*(3).
861 Keating-Bitonti, C. R., & Payne, J. L. (2018). Environmental influence on growth history in marine
862 benthic foraminifera. *Paleobiology*, *44*(4), 736–757. https://doi.org/10.1017/pab.2018.19
863 Kemp, A. C., Wright, A. J., & Cahill, N. (2020). Enough is Enough, or More is More? Testing the
864 Influence of Foraminiferal Count Size on Reconstructions of Paleo-Marsh Elevation. *Journal of*
865 *Foraminiferal Research*, *50*(3), 266–278. https://doi.org/10.2113/gsjfr.50.3.266
866 Levin, L. A., Ekau, W., Gooday, A. J., Jorissen, F., Middelburg, J. J., Naqvi, S. W. A., Neira, C.,
867 Rabalais, N. N., & Zhang, J. (2009). Effects of natural and human-induced hypoxia on coastal
868 benthos. *Biogeosciences*, *6*(10), 2063–2098. https://doi.org/10.5194/bg-6-2063-2009
869 McGann, M. (2011). Paleoceanographic changes on the Farallon Escarpment off central California during
870 the last 16,000 years. *Quaternary International*, *235*, 26–39.
871 https://doi.org/10.1016/j.quaint.2010.09.005
872 Moffitt, S. E., Hill, T. M., Ohkushi, K., Kennett, J. P., & Behl, R. J. (2014). Vertical oxygen minimum
873 zone oscillations since 20 ka in Santa Barbara Basin: A benthic foraminiferal community
874 perspective. *Paleoceanography*, *29*(1), 44–57. https://doi.org/10.1002/2013pa002483
875 Moffitt, S. E., Hill, T. M., Roopnarine, P. D., & Kennett, J. P. (2015). Response of seafloor ecosystems to
876 abrupt global climate change. *Proceedings of the National Academy of Sciences of the United*
877 *States of America*, *112*(15), 4684–4689. https://doi.org/10.1073/pnas.1417130112
878 Murgese, D. S., & De Deckker, P. (2005). The distribution of deep-sea benthic foraminifera in core tops
879 from the eastern Indian Ocean. *Marine Micropaleontology*, *56*(1), 25–49.
880 https://doi.org/10.1016/j.marmicro.2005.03.005
881 Myhre, S. E., Kroeker, K. J., Hill, T. M., Roopnarine, P., & Kennett, J. P. (2017). Community benthic
882 paleoecology from high-resolution climate records: Mollusca and foraminifera in post-glacial
883 environments of the California margin. *Quaternary Science Reviews*, *155*, 179–197.
884 https://doi.org/10.1016/j.quascirev.2016.11.009

885 Ohkushi, K., Kennett, J. P., Zeleski, C. M., Moffitt, S. E., Hill, T. M., Robert, C., Beaufort, L., & Behl, R.
886 J. (2013). Quantified intermediate water oxygenation history of the NE Pacific: A new benthic
887 foraminiferal record from Santa Barbara basin. *Paleoceanography*, *28*(3), 453–467.
888 https://doi.org/10.1002/palo.20043
889 Oksanen, J., Blanchet, F. G., Kindt, R., Legendre, P., Minchin, P. R., O'hara, R. B., Simpson, G. L.,
890 Solymos, P., Stevens, M. H. H., & Wagner, H. (2013). Package 'vegan.' *Community Ecology*
891 *Package, Version*, *2*(9).
892 Oschlies, A., Brandt, P., Stramma, L., & Schmidtko, S. (2018). Drivers and mechanisms of ocean
893 deoxygenation. *Nature Geoscience*, *11*(7), 467–473. https://doi.org/10.1038/s41561-018-0152-2
894 Palmer, H. M., Hill, T., Kennedy, E., Roopnarine, P., Langlois, S., Reyes, K., & Stott, L. (2022). *Data*
895 *from: Ecological and environmental stability in offshore Southern California Marine Basins*
896 *through the Holocene* (Version 6, p. 121877 bytes) [Data set]. Dryad.
897 https://doi.org/10.6071/M3Q090
898 Palmer, H. M., Hill, T. M., Roopnarine, P. D., Myhre, S. E., Reyes, K. R., & Donnenfield, J. T. (2020).
899 Southern California margin benthic foraminiferal assemblages record recent centennial-scale
900 changes in oxygen minimum zone. *Biogeosciences*, *17*(11), 2923–2937.
901 https://doi.org/10.5194/bg-17-2923-2020
902 Praetorius, S. K., Mix, A. C., Walczak, M. H., Wolhowe, M. D., Addison, J. A., & Prahl, F. G. (2015).
903 North Pacific deglacial hypoxic events linked to abrupt ocean warming. *Nature*, *527*(7578), 362-
904 +. https://doi.org/10.1038/nature15753
905 R Core Team. (2021). *R: A language and environment for statistical computing. R Foundation for*
906 *Statistical Computing*. https://www.R-project.org/
907 Rathburn, A. E., Willingham, J., Ziebis, W., Burkett, A. M., & Corliss, B. H. (2018). A New biological
908 proxy for deep-sea paleo-oxygen: Pores of epifaunal benthic foraminifera. *Scientific Reports*,
909 *8*(1), 9456. https://doi.org/10.1038/s41598-018-27793-4

910 Roark, E. B., Ingram, B. L., Southon, J., & Kennett, J. P. (2003). Holocene foraminiferal radiocarbon
911 record of paleocirculation in the Santa Barbara Basin. *Geology*, *31*(4), 379–382.
912 https://doi.org/Doi 10.1130/0091-7613(2003)031<0379:Hfrrop>2.0.Co;2
913 Schimmelmann, A., Hendy, I. L., Dunn, L., Pak, D. K., & Lange, C. B. (2013). Revised similar to 2000-
914 year chronostratigraphy of partially varved marine sediment in Santa Barbara Basin, California.
915 *Gff*, *135*(3–4), 258–264. https://doi.org/10.1080/11035897.2013.773066
916 Schmidtko, S., Stramma, L., & Visbeck, M. (2017). Decline in global oceanic oxygen content during the
917 past five decades. *Nature*, *542*(7641), 335-+. https://doi.org/10.1038/nature21399
918 Schmiedl, G., Mitschele, A., Beck, S., Emeis, K.-C., Hemleben, C., Schulz, H., Sperling, M., & Weldeab,
919 S. (2003). Benthic foraminiferal record of ecosystem variability in the eastern Mediterranean Sea
920 during times of sapropel S5 and S6 deposition. *Palaeogeography, Palaeoclimatology,*
921 *Palaeoecology*, *190*, 139–164. https://doi.org/10.1016/S0031-0182(02)00603-X
922 Schmiedl, G., Pfeilsticker, M., Hemleben, C., & Mackensen, A. (2004). Environmental and biological
923 effects on the stable isotope composition of recent deep-sea benthic foraminifera from the
924 western Mediterranean Sea. *Marine Micropaleontology*, *51*(1–2), 129–152.
925 Sharon, Belanger, C., Du, J., & Mix, A. (2021). Reconstructing Paleo-oxygenation for the Last 54,000
926 Years in the Gulf of Alaska Using Cross-validated Benthic Foraminiferal and Geochemical
927 Records. *Paleoceanography and Paleoclimatology*, *36*(2), e2020PA003986.
928 https://doi.org/10.1029/2020PA003986
929 Sharon, & Belanger, C. L. (2022). Placing North Pacific paleo-oxygenation records on a common scale
930 using multivariate analysis of benthic foraminiferal assemblages. *Quaternary Science Reviews*,
931 *280*, 107412. https://doi.org/10.1016/j.quascirev.2022.107412
932 Stott, L. D., Neumann, M., & Hammond, D. (2000). Intermediate water ventilation on the northeastern
933 Pacific margin during the late Pleistocene inferred from benthic foraminiferal delta C-13.
934 *Paleoceanography*, *15*(2), 161–169. https://doi.org/Doi 10.1029/1999pa000375

935 Stramma, L., Johnson, G. C., Firing, E., & Schmidtko, S. (2010). Eastern Pacific oxygen minimum zones:
936 Supply paths and multidecadal changes. *Journal of Geophysical Research: Oceans*, *115*(C9).
937 Stramma, L., Schmidtko, S., Levin, L. A., & Johnson, G. C. (2010). Ocean oxygen minima expansions
938 and their biological impacts. *Deep-Sea Research Part I-Oceanographic Research Papers*, *57*(4),
939 587–595. https://doi.org/10.1016/j.dsr.2010.01.005
940 Stuiver, M., & Polach, H. A. (1977). Discussion reporting of 14 C data. *Radiocarbon*, *19*(3), 355–363.
941 Talley, L. D. (1993). Distribution and Formation of North Pacific Intermediate Water. *Journal of Physical*
942 *Oceanography*, *23*(3), 517–537. https://doi.org/10.1175/1520-
943 0485(1993)023<0517:DAFONP>2.0.CO;2
944 Taylor, M. A., Hendy, I. L., & Pak, D. K. (2015). The California Current System as a transmitter of
945 millennial scale climate change on the northeastern Pacific margin from 10 to 50 ka.
946 *Paleoceanography*, *30*(9), 1168–1182. https://doi.org/10.1002/2014pa002738
947 Tetard, M., Licari, L., Tachikawa, K., Ovsepyan, E., & Beaufort, L. (2021). Toward a global calibration
948 for quantifying past oxygenation in oxygen minimum zones using benthic Foraminifera.
949 *Biogeosciences Discussions*, 1–17. https://doi.org/10.5194/bg-2020-482
950 Venturelli, R. A., Rathburn, A., Burkett, A., & Ziebis, W. (2018). Epifaunal Foraminifera in an Infaunal
951 World: Insights Into the Influence of Heterogeneity on the Benthic Ecology of Oxygen-Poor,
952 Deep-Sea Habitats. *Frontiers in Marine Science*, *5*, 344.
953 Wang, Y., Hendy, I. L., & Zhu, J. (2020). Expansion of the Southern California oxygen minimum zone
954 during the early-to mid-Holocene due to reduced ventilation of the Northeast Pacific. *Quaternary*
955 *Science Reviews*, *238*, 106326. https://doi.org/10.1016/j.quascirev.2020.106326
956

Paleoceanography and Paleoclimatology

Supporting Information for

Ecological and environmental stability in offshore Southern California Marine Basins through the Holocene

Hannah M. Palmer[1,2], Tessa M. Hill[1,2], Esther G. Kennedy[1,2], Peter Roopnarine[3], Sonali Langlois[4], Katherine R. Reyes[5], and Lowell Stott[6]

1. Earth and Planetary Sciences, University of California, Davis
2. Bodega Marine Laboratory, University of California, Davis
3. California Academy of Sciences
4. Santa Rosa Junior College
5. Dominican University of California
6. University of Southern California

Contents of this file

Introduction

Supporting information contains five supporting figures and two supporting tables. All methodology is discussed in main text.

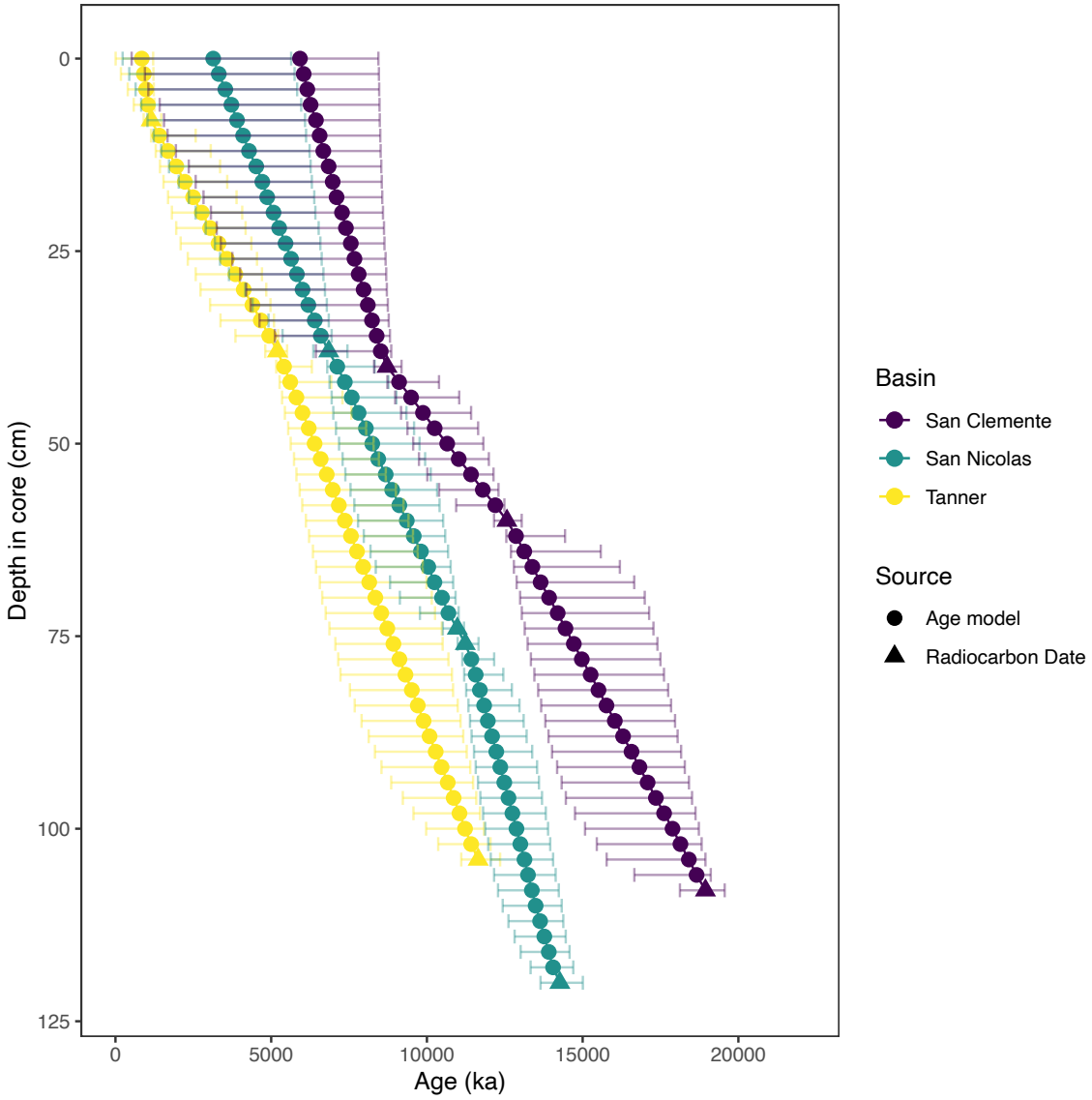

Figure S1. Radiocarbon-based age model as generated through Bchron for three cores included in study. Age shown in thousands of years before present. Triangles are calibrated radiocarbon ages, circles are median ages generated through Bchron age model: Tanner= yellow, San Nicolas = green, San Clemente = purple). Error bars indicate 95% credible interval at each depth.

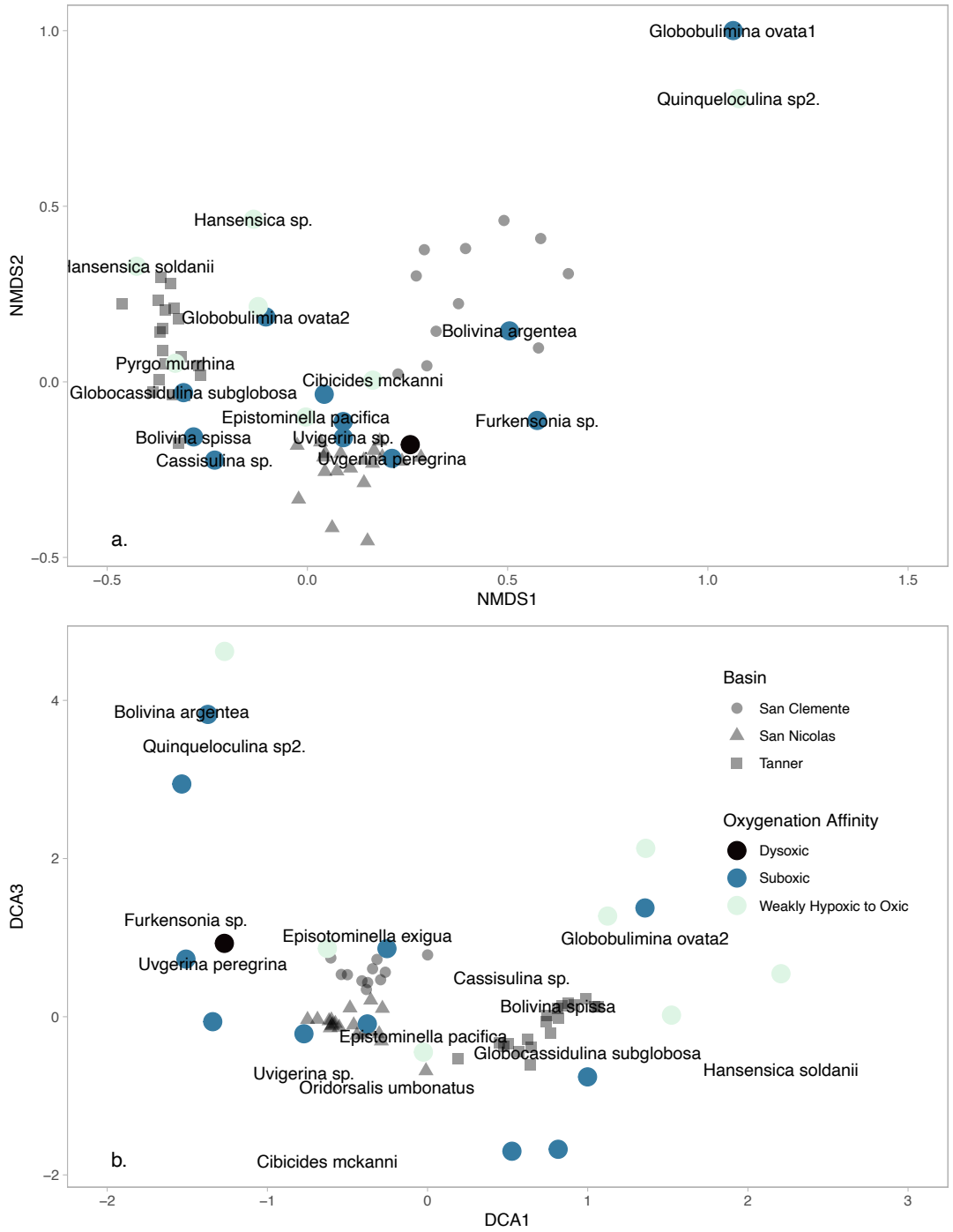

Figure S2. Non-metric multidimensional scaling plot (a.) and detrended correspondence plot (b.) of all benthic foraminiferal assemblages through time from three cores. Axes that represent the most variance are shown here. Species are large circles color coded by published oxygenation affinity (dark blue is dysoxic, blue is suboxic, and teal gray is weakly hypoxic to oxic). All other points represent assemblages at each interval through time at each of the three cores; gray dots are San Clemente assemblage, gray triangles are San Nicolas assemblage, and gray squares are Tann assemblage.

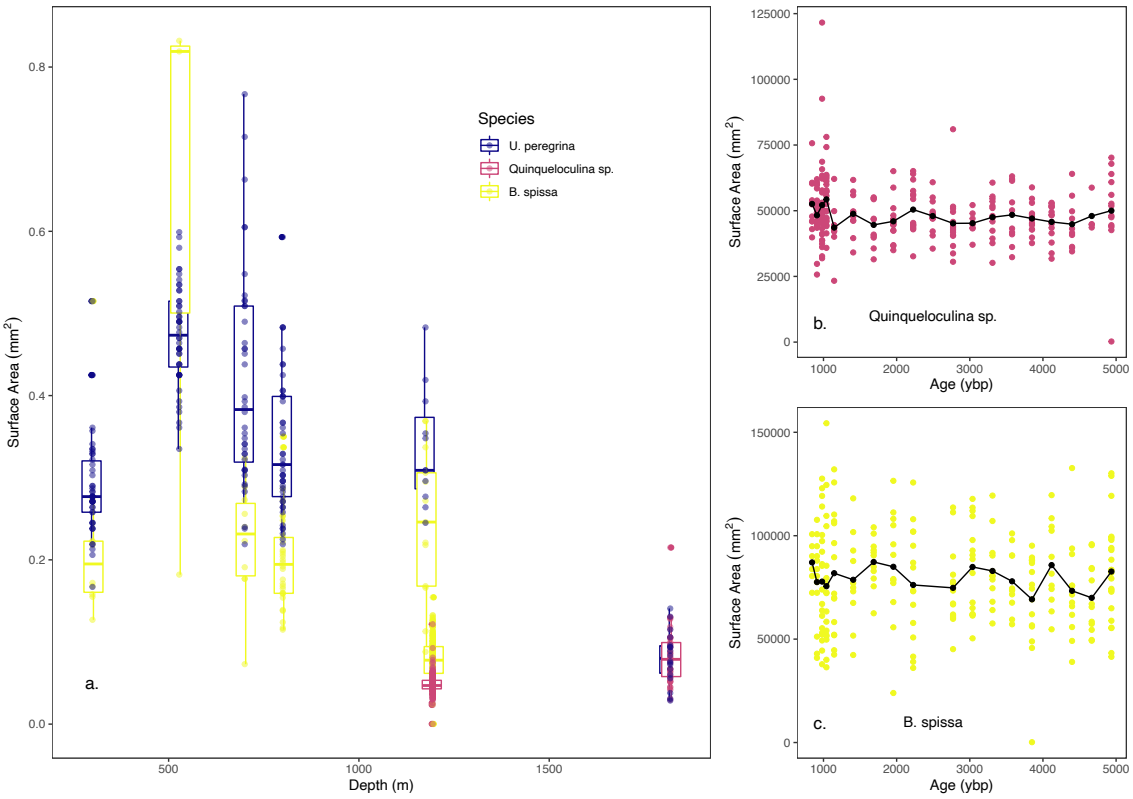

Figure S3. Shell surface area (mm^2) vs. water depth (m) at all points in time (a.). Data shown here indicate all points in time from each water depth. Colors represent species: U. peregrina = purple, *Quinqueloculina* sp. = magenta, *B. spissa* = yellow. All points are shown in addition to box plot. Box plot is slightly offset to better display two species at each water depth. Surface area of *Quinqueloculina* sp. (b.) and *B. spissa* (c.) vs. time in years before present from Tanner Basin.

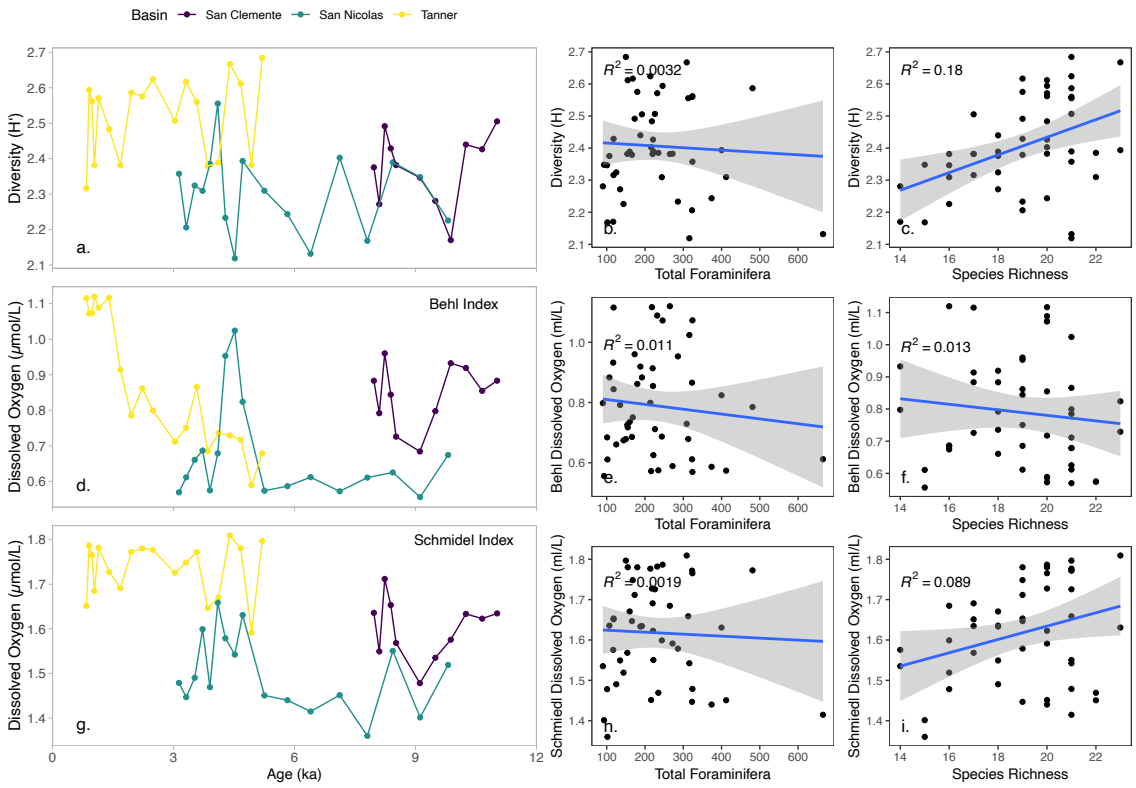

Figure S4. Diversity (Shannon Index), vs. age in thousands of years before present (a.), total foraminifera (b.), and species richness (c.). Reconstructed dissolved oxygen (ml/L) using Behl Index vs. age in thousands of years before present (a.), total foraminifera (b.), and species richness (c.). Reconstructed dissolved oxygen (ml/L) using Schmiedl Index vs. age in thousands of years before present (a.), total foraminifera (b.), and species richness (c.). Trendlines in panels b., c., e., f., h., and i., use linear regression, R^2 is shown on plot.

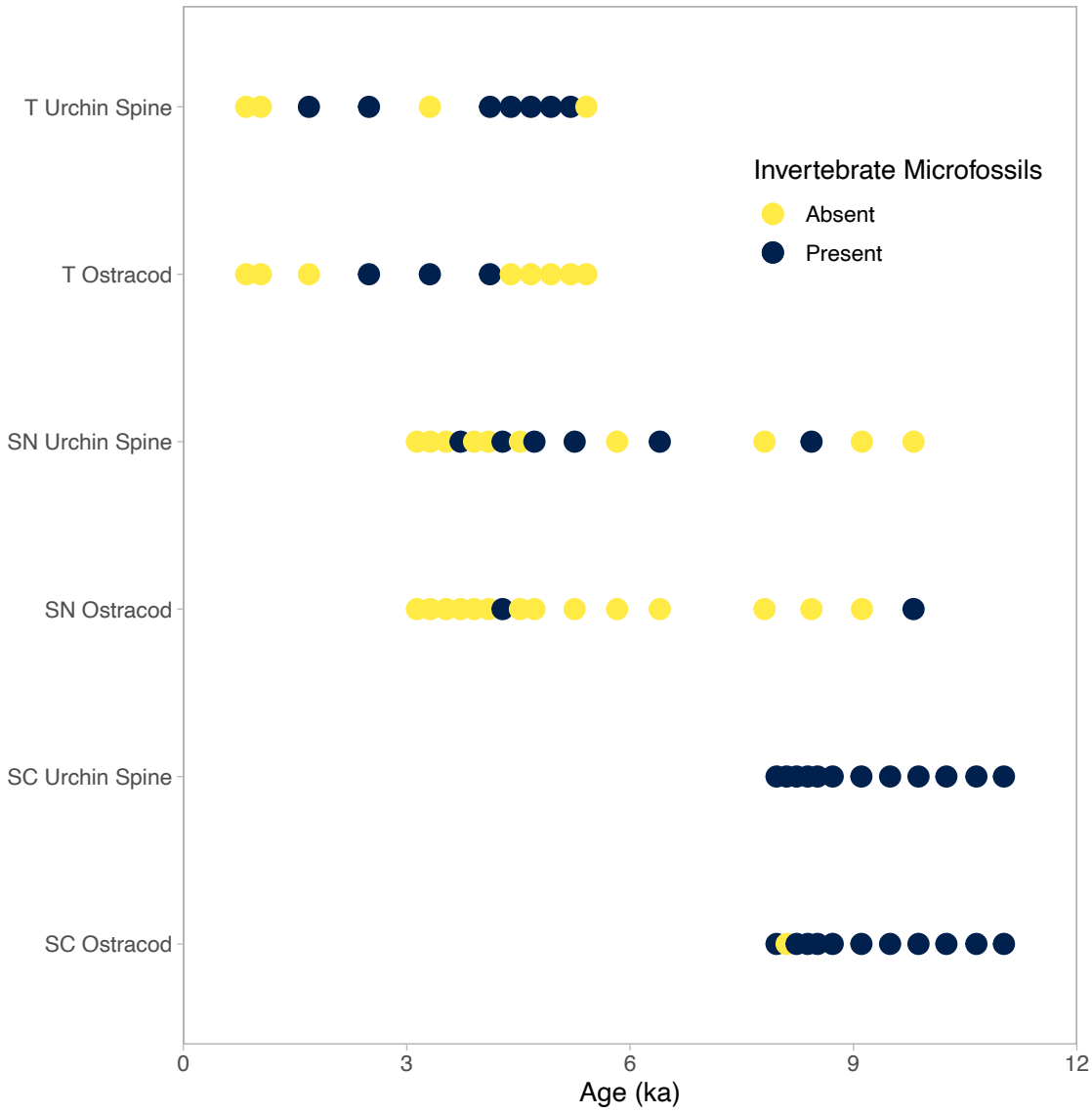

Figure S5: Presence and absence of metazoan microfossils (urchin spines and ostracods) through time (age in thousands of years before present) for each basin (Tanner (T), San Nicolas (SN), and San Clemente (SC)). Presence is blue, absence is yellow.

Basin	**Core**	**Sample Interval**	**Source**	**Radiocarbon date** (14C years)	**±**	**Calendar age** (years before present)	**95% Credible Interval** (years before present)
Tanner	EW95 04-09	8-10 cm	Stott et al., 2000	1950	50	1146	905-1468
Tanner	EW95 04-09	38- 40 cm	This paper	5290	30	5201	4809-5511
Tanner	EW95 05-09	104-106 cm	Stott et al., 2000	10790	60	11647	11102-12350
San Nicolas	EW95 04-08	38-40 cm	Stott et al., 2000	6780	50	6849	6351-7448
San Nicolas	EW95 04-08	74-76 cm	This paper	10330	35	10976	10511-11190
San Nicolas	EW95 04-08	76-78 cm	Stott et al., 2000	10460	70	11233	10987-11657
San Nicolas	EW95 04-08	120-122 cm	Stott et al., 2000	12870	160	14269	13647-15006
San Clemente	EW95 04-08	40-42 cm	Stott et al., 2000	8550	60	8721	8308-9185
San Clemente	EW95 04-08	60-62 cm	This paper	11430	40	12570	12155-13043
San Clemente	EW95 04-08	108-110 cm	Stott et al., 2000	16650	50	18942	181123-19560

Table S1. Radiocarbon ages and age model for all three cores examined here. Radiocarbon age calibrated using reservoir age of 220 +- 40 and Bchron Bayesian approach.

Species	Oxygen Classification	Modified from Sharon-Behl	Citation for oxygenation affinity
Bolivina argentea	Suboxic		Sharon et al., 2021
Bolivina pseudobeyrichi	Dysoxic		Sharon et al., 2021
Bolivina spissa	Suboxic		Sharon et al., 2021
Bulimina tenuata	Dysoxic		Sharon et al., 2021
Cassidulina sp.	Suboxic		Sharon et al., 2021
Chlistomella ovoidea	Suboxic		Sharon et al., 2021
Cibicides mckannai	Weakly hypoxic to oxic	Modified	Kaiho 1994
Cibicides sp.	Weakly hypoxic to oxic	Modified	Kaiho 1994
Elphidium sp.	Weakly hypoxic to oxic		Sharon et al., 2021
Epistominella exigua	Suboxic		Sharon et al., 2021
Epistominella pacifica	Weakly hypoxic to oxic	Modified	Cannariato and Kennett 1999
Fursenkoina sp.	Suboxic	Modified	Kaiho 1994
Globobulimina barbata	Suboxic	Modified	Ohkushi et al., 2013
Globobulimina ovata1	Suboxic	Modified	Ohkushi et al., 2013
Globobulimina ovata2	Suboxic	Modified	Ohkushi et al., 2013
Globobulimina pacifica	Suboxic	Modified	Ohkushi et al., 2013
Globocassidulina sp.	Suboxic		Sharon et al., 2021
Globocassidulina subglobosa	Suboxic		Sharon et al., 2021
Hansenisca soldanii	Weakly hypoxic to oxic	Modified	De and Gupta 2010
Hansenisca sp.	Weakly hypoxic to oxic	Modified	De and Gupta 2010
Melonis affinis	Suboxic	Modified	Kaiho 1994
Nonionella stella	Dysoxic		Sharon et al., 2021
Oridorsalis umbonatus	Suboxic		Sharon et al., 2021
Other			
Pyrgo murrhina	Weakly hypoxic to oxic		Sharon et al., 2021
Quinqueloculina sp.	Weakly hypoxic to oxic		Sharon et al., 2021
Quinqueloculina sp2.	Weakly hypoxic to oxic		Sharon et al., 2021
Uvigerina peregrina	Suboxic		Sharon et al., 2021
Uvigerina proboscoidea	Suboxic		Sharon et al., 2021
Uvigerina sp.	Suboxic		Sharon et al., 2021

Table S2. Oxygen affinity for all species examined here and utilized in oxygen transfer functions.

	NMDS1 (43.0%)	NMDS2 (15.8%)	NMDS3 (3.1%)	NMDS4 (0.8%)
Bolivina spissa	-0.284	-0.157	0.167	-0.042
Cassisulina sp.	-0.232	-0.223	0.080	-0.085
Cibicides mckanni	0.163	0.005	-0.153	0.166
Epistominella pacifica	-0.004	-0.100	-0.046	0.122
Episotominella exigua	0.089	-0.113	-0.040	-0.059
Globobulimina ovata2	-0.104	0.185	0.005	-0.089
Globocassidulina subglobosa	-0.309	-0.031	0.045	0.033
Hansensica soldanii	-0.427	0.329	-0.075	0.076
Oridorsalis umbonatus	0.042	-0.035	-0.123	0.103
Pyrgo murrhina	-0.330	0.053	-0.007	0.049
Quinqueloculina sp.	-0.123	0.214	0.101	-0.041
Uvigerina sp.	0.090	-0.159	-0.068	0.038
Uvgerina peregrina	0.211	-0.218	-0.028	0.004
Hansensica sp.	-0.135	0.463	-0.357	-0.239
Nonionella stella	0.257	-0.179	-0.072	-0.141
Bolivina argentea	0.505	0.145	-0.813	-0.953
Furkensonia sp.	0.574	-0.110	0.239	0.125
Quinqueloculina sp2.	1.077	0.806	0.276	-0.216
Globobulimina ovata1	1.063	1.000	0.611	0.317

Table S3. NMDS species scores. Proportion of variance for each axis is reported in parenthetical. Proportion of variance of each axis was calculated summarized by each axis using the Pearson correlation between the Euclidean dissimilarity of the sites scores and the Bray-Curtis dissimilarity of the faunal abundances for each site with the mantel function in the "ecodist" package (Sharon et al., 2021).

	DCA1 (45.6%)	DCA2 (6.2%)	DCA3 (11.3%)	DCA4 (2.1%)
Bolivina spissa	0.815	0.132	-1.676	-0.235
Cassisulina sp.	0.527	0.490	-1.701	-0.720
Cibicides mckanni	-0.626	-1.833	0.864	0.333
Epistominella pacifica	-0.026	-0.248	-0.447	1.073
Episotominella exigua	-0.376	1.024	-0.091	-1.480
Globobulimina ovata2	1.358	0.997	1.375	-1.259
Globocassidulina subglobosa	0.999	-0.456	-0.761	-0.038
Hansensica soldanii	2.207	-0.665	0.544	0.706
Oridorsalis umbonatus	-0.253	-0.897	0.861	-0.859
Pyrgo murrhina	1.523	-0.763	0.020	0.498
Quinqueloculina sp.	1.124	0.525	1.273	1.365
Uvigerina sp.	-0.772	-0.713	-0.215	0.231
Uvgerina peregrina	-1.341	0.669	-0.063	0.199
Hansensica sp.	1.362	-0.780	2.129	-2.557
Nonionella stella	-1.269	1.092	0.928	0.723
Bolivina argentea	-1.535	3.864	2.943	1.728
Furkensonia sp.	-1.508	1.231	0.729	1.057
Quinqueloculina sp2.	-1.267	3.421	4.619	2.955
Globobulimina ovata1	-1.372	3.262	3.822	4.412

Table S4. DCA species scores. Proportion of variance for each DCA axis is reported in parenthetical. Proportion of variance of each axis was calculated summarized by each axis using the Pearson correlation between the Euclidean dissimilarity of the DCA sites scores and the Bray-Curtis dissimilarity of the faunal abundances for each site with the mantel function in the "ecodist" package (Sharon et al., 2021).